28. Seki T, Ota M, Furuta S, Fukushima H, Kondo T, Hino K, et al. HLA class II molecules and autoimmune hepatitis susceptibility in Japanese patients. Gastroenterology. 1992;103:1041–7.
29. Kawa S, Ota M, Yoshizawa K, Horiuchi A, Hamano H, Ochi Y, et al. HLA DRB10405-DQB10401 haplotype is associated with autoimmune pancreatitis in the Japanese population. Gastroenterology. 2002;122:1264–9.
30. Umemura T, Ota M, Yoshizawa K, Katsuyama Y, Ichijo T, Tanaka E, et al. Association of cytotoxic T-lymphocyte antigen 4 gene polymorphisms with type 1 autoimmune hepatitis in Japanese. Hepatol Res. 2008;38:689–95.
31. Umemura T, Ota M, Hamano H, Katsuyama Y, Muraki T, Arakura N, et al. Association of autoimmune pancreatitis with cytotoxic T-lymphocyte antigen 4 gene polymorphisms in Japanese patients. Am J Gastroenterol. 2008;103:588–94.
32. Umemura T, Ota M, Yoshizawa K, Katsuyama Y, Ichijo T, Tanaka E, et al. Lack of association between FCRL3 and FcgammaRII polymorphisms in Japanese type 1 autoimmune hepatitis. Clin Immunol. 2007;122:338–42.
33. Umemura T, Ota M, Hamano H, Katsuyama Y, Kiyosawa K, Kawa S. Genetic association of Fc receptor-like 3 polymorphisms with autoimmune pancreatitis in Japanese patients. Gut. 2006;55:1367–8.

European Journal of Radiology 76 (2010) 228–238

Contents lists available at ScienceDirect

European Journal of Radiology

journal homepage: www.elsevier.com/locate/ejrad

Characteristic findings in images of extra-pancreatic lesions associated with autoimmune pancreatitis☆

Yasunari Fujinaga[a,*], Masumi Kadoya[a], Shigeyuki Kawa[b], Hideaki Hamano[c], Kazuhiko Ueda[a], Mitsuhiro Momose[a], Satoshi Kawakami[a], Sachie Yamazaki[a], Tomoko Hatta[a], Yukiko Sugiyama[a]

[a] Department of Radiology, Shinshu University School of Medicine, 3-1-1 Asahi, Matsumoto, 390-8621, Japan
[b] Center of Health, Safety and Environmental Management, Shinshu University School of Medicine, 3-1-1 Asahi, Matsumoto, 390-8621, Japan
[c] Department of Medicine, Gastroenterology, Shinshu University School of Medicine, 3-1-1 Asahi, Matsumoto, 390-8621, Japan

ARTICLE INFO

Article history:
Received 21 January 2009
Accepted 9 June 2009

Keywords:
Autoimmune pancreatitis
Extra-pancreatic lesions
Computed tomography
Magnetic resonance imaging
Gallium scintigraphy

ABSTRACT

Purpose: Autoimmune pancreatitis is a unique form of chronic pancreatitis characterized by a variety of extra-pancreatic involvements which are frequently misdiagnosed as lesions of corresponding organs. The purpose of this study was to clarify the diagnostic imaging features of extra-pancreatic lesions associated with autoimmune pancreatitis.

Materials and methods: We retrospectively analyzed diagnostic images of 90 patients with autoimmune pancreatitis who underwent computer-assisted tomography, magnetic resonance imaging, and/or gallium-67 scintigraphy before steroid therapy was initiated.

Results: AIP was frequently (92.2%) accompanied by a variety of extra-pancreatic lesions, including swelling of lachrymal and salivary gland lesions (47.5%), lung hilar lymphadenopathy (78.3%), a variety of lung lesions (51.2%), wall thickening of bile ducts (77.8%), peri-pancreatic or para-aortic lymphadenopathy (56.0%), retroperitoneal fibrosis (19.8%), a variety of renal lesions (14.4%), and mass lesions of the *ligamentum teres* (2.2%). Characteristic findings in CT and MRI included lymphadenopathies of the hilar, peri-pancreatic, and para-aortic regions; wall thickening of the bile duct; and soft tissue masses in the kidney, ureters, aorta, paravertebral region, *ligamentum teres*, and orbit.

Conclusions: Recognition of the diagnostic features in the images of various involved organs will assist in the diagnosis of autoimmune pancreatitis and in differential diagnoses between autoimmune pancreatitis-associated extra-pancreatic lesions and lesions due to other pathologies.

1. Introduction

Autoimmune pancreatitis (AIP) is a unique form of chronic pancreatitis characterized by a preponderance of elderly male sufferers, minimal abdominal pain, irregular narrowing of the main pancreatic duct, and swelling of the pancreatic parenchyma [1–12]. The pathogenesis is thought to involve an autoimmune mechanism based on the presence of various serum autoantibodies, hypergammaglobulinemia, histological evidence of lymphoplasmacytic inflammation and fibrosis, and a favorable response to glucocorticoid treatment [13–21]. This disease has been occasionally misdiagnosed as pancreatic cancer, leading to unnecessary surgery [22,23]. It is therefore imperative to improve the diagnostic accuracy for AIP.

The characteristic features of AIP include a high serum IgG4 concentration and complications involving various extra-pancreatic lesions. Over 90% of patients exhibit high serum IgG4 concentrations, reflecting infiltration of abundant IgG4-bearing plasma cells and disease activity [11] in the pancreatic lesion [12,18]. Thus, a serum assay for IgG4 provides a useful tool for the diagnosis and monitoring of this disease. In addition, abundant IgG4-bearing plasma cells are a histological hallmark that can be used in differentiating between AIP and malignant conditions.

Other prominent features of AIP involve a variety of extra-pancreatic complications, including sclerosing cholangitis [2,7,17,19,20], lachrymal and salivary gland abnormalities [18,24], hypothyroidism [25], hilar lymphadenopathy [26], retroperitoneal fibrosis [12,17,27–29], interstitial pneumonia [30,31], and tubulointerstitial nephritis [32,33]. Some of these extra-pancreatic lesions exhibit pathologies similar to those found in pancreatic lesions, including infiltration of abundant IgG4-bearing plasma

Abbreviations: AIP, autoimmune pancreatitis; CT, computer-assisted tomography; Ga-67, gallium-67; LIP, lymphocytic interstitial pneumonia; MRI, magnetic resonance imaging; MRCP, magnetic resonance cholangiopancreatography; NSIP, nonspecific interstitial pneumonia; PSC, primary sclerosing cholangitis.

☆ This work was supported in part by Grants-in-aid for Scientific Research from the Ministry of Education, Science, Sports and Culture of Japan (20590805).

* Corresponding author. Tel.: +81 263 37 2650; fax: +81 263 37 3087.
E-mail address: fujinaga@shinshu-u.ac.jp (Y. Fujinaga).

0720-048X/$ – see front matter © 2009 Elsevier Ireland Ltd. All rights reserved.
doi:10.1016/j.ejrad.2009.06.010

cells [12,18,26,29]. In addition, the presence of multiple extra-pancreatic lesions suggests a systemic disease associated with IgG4 [12]. Most reports regarding AIP-associated extra-pancreatic lesions have been published as single cases, small series of cases, or cases restricted to specific lesions. There have been only a few detailed reports addressing the broad spectrum of manifestations [34,35,36], particularly with regard to imaging that might be useful in the diagnosis of extra-pancreatic lesions associated with AIP.

It is uncertain whether there are imaging characteristics that might be useful for differentiation between IgG4-related extra-pancreatic lesions and other diseases affecting the same organs. In this study, we aimed to characterize and identify useful imaging features of a large cohort in the diagnosis of extra-pancreatic manifestations of AIP to differentiate them from other diseases affecting the same organs.

2. Materials and methods

We systematically reviewed diagnostic images for 90 patients with AIP, 75 men and 15 women aged 38–79 (median age, 63.1 years old), treated in our hospital and affiliated hospitals between September, 1994 and March, 2008. Diagnosis of AIP was based on the criteria proposed by the Japanese Pancreatic Society in 2002 [37] and the revised version in 2006 [38].

We analyzed images from computer-assisted tomography (CT), magnetic resonance imaging (MRI), and/or gallium-67 (Ga-67) scintigraphy that were taken at admission or during an active stage of the disease before the initiation of steroid therapy. CT examination was performed with single-detector row helical CT (HiSpeed Advantage; GE Medical Systems, Milwaukee, WI, USA) from 1994 to 2003 and with multi-detector row helical CT from 2003 to 2008 (LightSpeed Ultra or LightSpeed VCT; GE Medical Systems, Milwaukee, WI, USA). Because of the length of the period under review, the model of the CT scanner, slice thickness (1.25–10 mm) and the protocol of the contrast-enhanced CT varied. MRI was performed with a 1.5-T superconductor unit (Magnetom Symphony, Siemens Medical Solution, Erlangen, Germany) from 1994 to 2006 and with a 3-T superconductor unit (Magnetom Trio, Siemens Medical Solution, Erlangen, Germany) from 2007 to 2008. The slice thickness (2–10 mm), image sequence and the protocol of the contrast-enhanced MRI varied for the same reason. Ga-67 scintigraphy was performed with a single-head rectangular gamma camera (SNC-510R; Shimazu, Japan) from 1994 to 2002 and a triple-head rotating gamma camera (PRISM IRIX; Philips Medical Systems, Best, The Netherlands) or a large field-of-view dual-detector gamma camera with a mounted CT scanner (Millennium VG, GE Medical Systems, Milwaukee, WI, USA) from 2003 to 2008.

Abdominal and thoracic CT images were available in all 90 and 69 patients, respectively. Abdominal MRI and neck MRI were available in 78 and 40 patients, respectively. Ga-67 scintigram was available in 80 patients. Systemic image analysis using CT, MRI and Ga-67 was performed, even if they showed no specific symptoms of the extra-pancreatic organs, because lesions in extra-pancreatic organs found on images were not always associated with symptoms. Image findings were reviewed by two radiologists (Y.F. and M.K.) in consensus.

Table 1
Summary of the prevalence and distribution of extra-pancreatic lesions.

Organ	No. of cases	Percentage
Total extra-pancreatic lesions	83/90	92.2%
Lachrymal or salivary grand	38/80	47.5%
Hilar lymph node (CT)	54/69	78.3%
Hilar lymph node (Ga-67 scintigraphy)	60/80	75%
Lung	25/46	54.3%
Bile duct	63/81	77.8%
Peri-pancreatic or para-aortic lymph node	51/90	57%
Kidneys	13/90	14.4%
Retroperitoneum	17/86	19.8%
Ligamentum teres	2/90	2.2%
Prostate	8/80	10.0%

The total number of examined cases in each row is different among respective lesions because CT, MRI or Ga-67 scintigraphy were not performed in all the organs, and some images were not available.

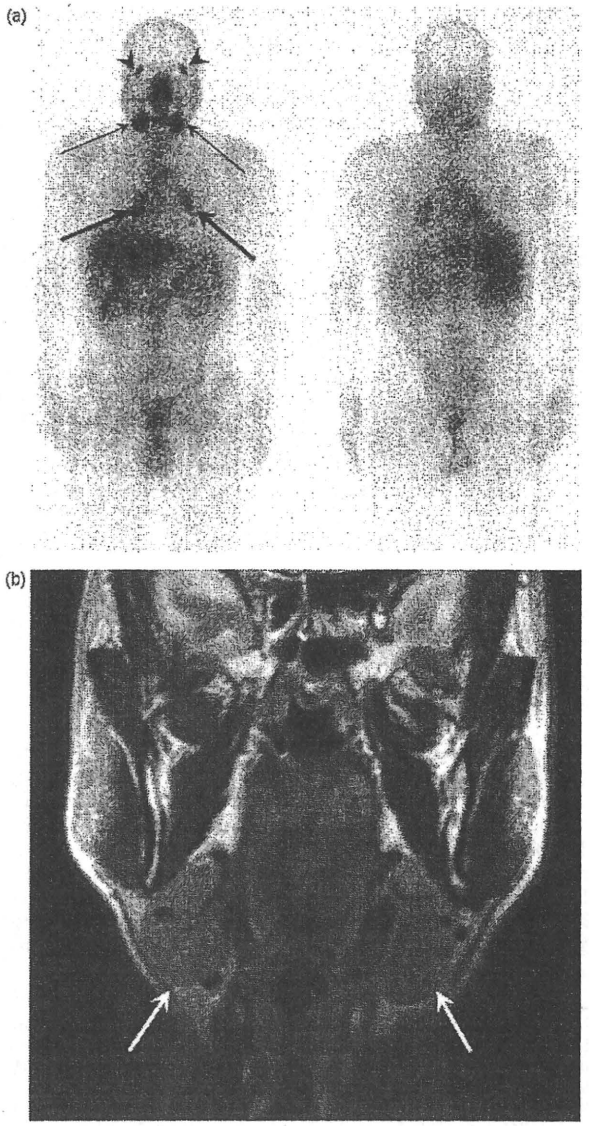

Fig. 1. Lachrymal and salivary lesions in a 67-year-old man visualized with Ga-67 scintigraphy and MRI. (a) Ga-67 scintigraphy shows increased uptake in the hilar (arrows), submandibular (thin arrows), and lachrymal glands (arrow heads). (b) Coronal T2-weighted images show bilateral submandibular gland swellings that are homogeneous without dilatation of the ducts (white arrows).

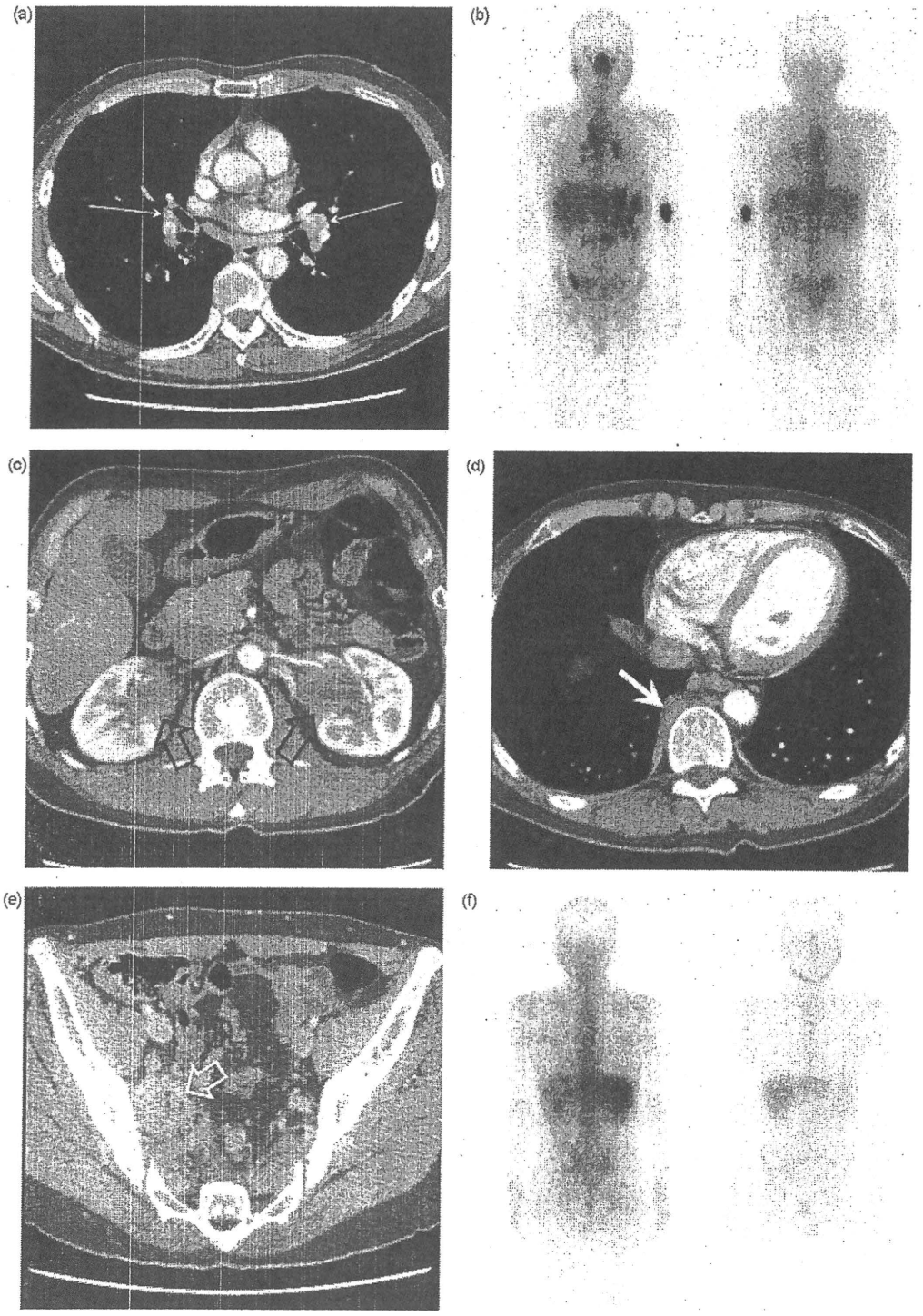

Fig. 2. Hillar lymphadenopathy in a 50-year-old man. (a) Dynamic contrast-enhanced CT shows hilar lymphadenopathy (long arrows). (b) Ga-67 scintigraphy demonstrates an increased uptake in right parotid gland and right retroperitoneum, as well as hilum. (c–e) Another slice of the dynamic contrast-enhanced CT identifies bilateral renal lesions (open arrows in c), paravertebral mass (white arrow in d) and retroperitoneal lesion (white open arrow in e) (to be describe). (f) After corticosteroid therapy, the accumulation of Ga-67 disappeared in each lesion.

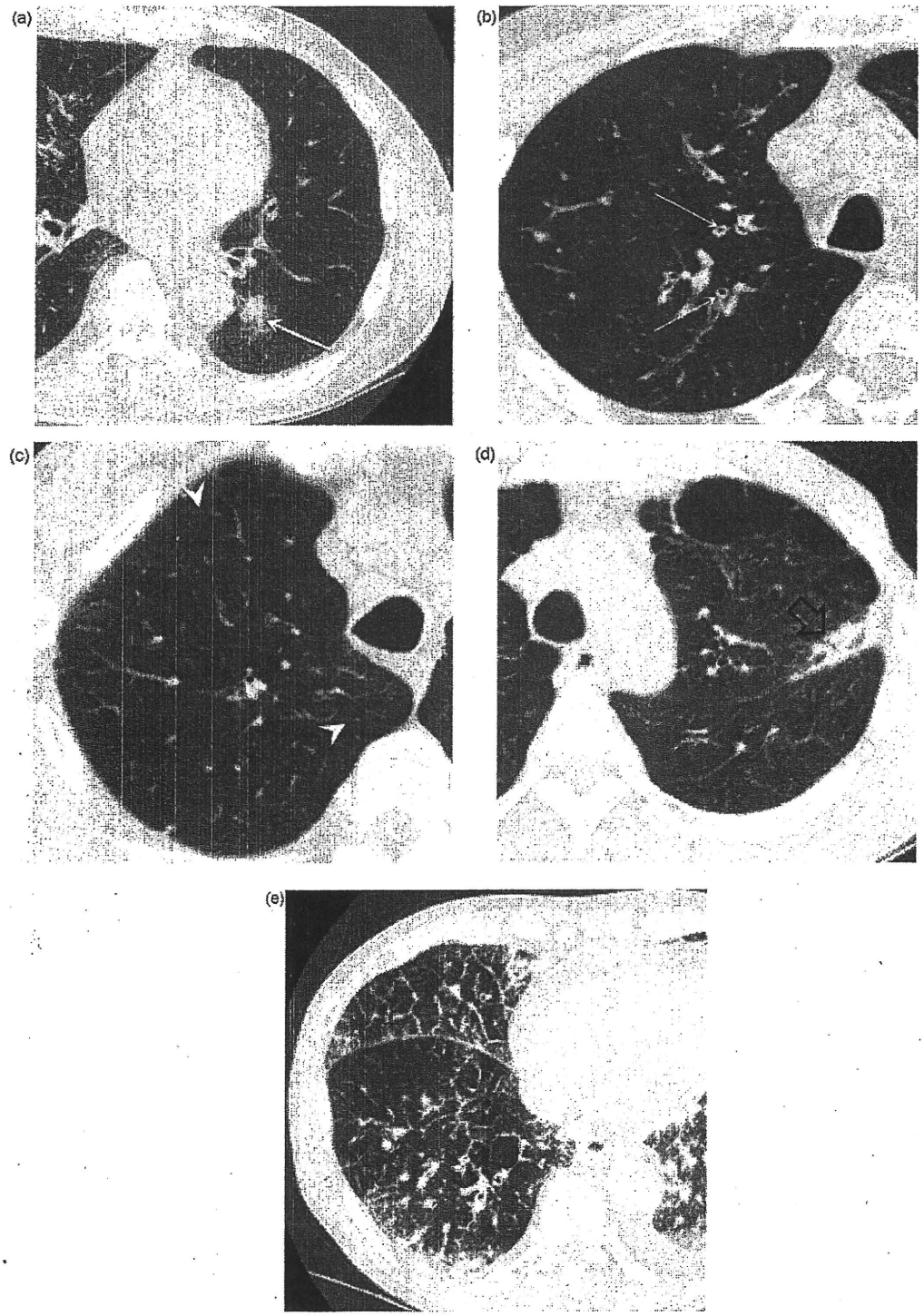

Fig. 3. Lung lesions. (a–d) Thin-sliced CT before corticosteroid therapy shows an irregular nodular lesion in the left lower lobe (white arrow in a), bronchial thickening in the right upper lobe (thin white arrows in b), diffuse interlobular thickening in the right upper lobe (arrow heads in c), and subpleural consolidation in the left lower lobe (open arrow in d). (e) In another case, a coarse reticulation consistent with thickening of interlobular septa is mixed with multiple subpleural consolidations in the right lower lobe.

Fig. 4. Bile duct lesions in a 50-year-old woman. Coronal reformation of contrast-enhanced CT shows marked bile duct wall thickening (arrows).

3. Results

Among 90 patients, 83 (92.2%) had various extra-pancreatic lesions associated with AIP. We summarize the distribution and frequency of the extra-pancreatic lesions in Table 1, and describe the details of each type of lesion in the following sections.

3.1. Lachrymal and salivary gland lesions

Among 80 patients that underwent Ga-67 scintigraphy, 38 (47.5%) had lachrymal or salivary gland lesions (Table 1). Two submandibular lesions and two lachrymal lesions were histopathologically proven by biopsy, and other lesions were clinically diagnosed. Ga-67 scintigraphy showed increased uptake in either the lachrymal or salivary gland in 36 of these 38 patients (95%) (Fig. 1a). The submandibular gland was involved in 29 patients (76%), the lachrymal gland in 27 (75%), the parotid gland in 5 (13%), and the sublingual gland in 2 (5%). Increased uptakes were symmetrical in all except three of the patients; one showed right-side-dominant uptake at the lachrymal gland, one showed left-side-dominant uptake at the lachrymal gland, and one showed right-side-dominant uptake at the submandibular gland. After corticosteroid therapy, increased uptake of all lesions was disappeared.

Neck MRI was performed in 40 patients in whom increased uptake was seen on Ga-67 scintigraphy or clinical symptoms were described. The MRIs showed a bilateral homogeneous swelling of the glands without a discernable mass (Fig. 1b) in 14 patients, unilateral swelling in 2 patients and normal findings in 24 patients. Biopsies performed in two patients showed that the swelling submandibular glands contained abundant IgG4-bearing plasma cells. No lesions showed the salt-and-pepper appearance characteristic of Sjoegren's syndrome [39].

3.2. Hilar lymphadenopathy

Hilar lymphadenopathy was revealed in 54 of 69 patients (78%) undergoing thoracic CT (Table 1), and contrast-enhanced CT was used to improve the visualization of bilateral hilar lymphadenopathy (Fig. 2a). Ga-67 scintigraphy also showed marked bilateral hilar uptake in 60 of 80 cases (75%) (Fig. 2b) (Table 1). After corticosteroid therapy, bilateral hilar lymphadenopathy disappeared in all cases. No biopsies were taken. There was no unilateral lymphadenopathy found by CT or Ga-67 scintigraphy.

3.3. Pulmonary abnormalities

Lung lesions were revealed in 25 of 46 patients (54%) undergoing thin-slice CT (Table 1). Five patients were histopathologically

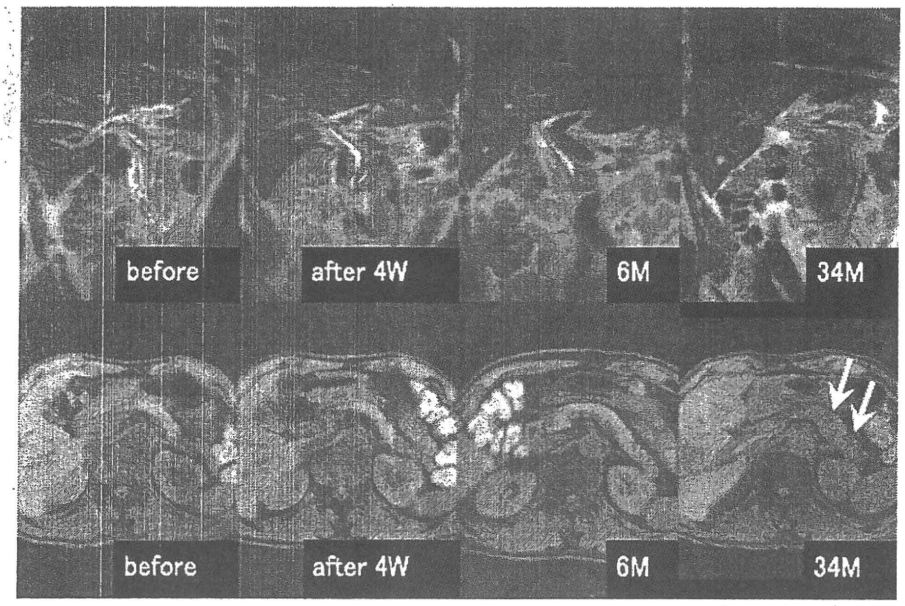

Fig. 5. Bile duct lesions in a 69-year-old man. Oblique coronal T2-weighted images (upper column) before and after corticosteroid therapy images show gradual improvement of the bile duct lesion. Thirty-four months after corticosteroid therapy, the bile duct lesion had relapsed. Axial fat saturated T1-weighted images (lower column) show a new pancreatic lesion (white arrows) accompanied by relapsed bile duct lesion.

proven by biopsy and 20 were clinically diagnosed. There were four types of CT findings, including nodular lesions, bronchial thickening, interlobular thickening, and consolidation. Nodular lesions (3–26 mm in diameter) were found in 18 (39%) (Fig. 3a), bronchial thickening in 14 (30%) (Fig. 3b), interlobular thickening in 7 (15%) (Fig. 3c), and consolidations in 2 (4%) (Fig. 3d). Almost all the nodular lesions were located adjacent to the pleura. Two or more types of lesions coexisted in 14 cases (Fig. 3e). All lesions diminished or disappeared after corticosteroid therapy.

3.4. Bile duct abnormalities

CT or MRI showed extra-pancreatic bile duct lesions in 63 of 81 patients (78%) (Table 1); nine patients were excluded due to unavailable CT or MR images, or if the detailed analysis of bile ducts was difficult due to occlusion by drainage tubes. Biopsies were performed in 19 cases, and abundant IgG4-bearing plasma cell infiltration was evident. Other 44 cases were clinically diagnosed. Almost all bile duct abnormalities in these 63 patients included extensive wall thickening, with occlusion of the intrahepatic bile duct in 23 (28%) and of the common hepatic or intra-pancreatic common bile duct in 37 (46%) (Fig. 4). MRI clearly demonstrated these lesions (Fig. 5), and showed prominent wall thickening with a laminar structure (Fig. 6) in some cases and focal wall thickening of the common bile duct in 5 (6%). Magnetic resonance cholangiopancreatography (MRCP) was performed in 66 patients and showed intrahepatic bile duct stenosis, which mimicked primary sclerosing cholangitis (PSC) in 6 (9%). Severe bile duct dilatation was observed when the pancreas head was swollen.

3.5. Peri-pancreatic and para-aortic lymphadenopathy

CT or MRI showed peri-pancreatic or para-aortic lymphadenopathy in 51 of 90 cases (57%) (Table 1). All lesions were clinically diagnosed. CT clearly demonstrated lymph node swelling that produced high signal intensities on diffusion-weighted MRI (Fig. 7a, b). No biopsies were taken, but corticosteroid therapy was effective for all lesions.

Fig. 6. Bile duct lesions in a 50-year-old woman. Coronal contrast-enhanced MRI shows prominent wall thickening of the bile duct with significant laminar structure (arrows).

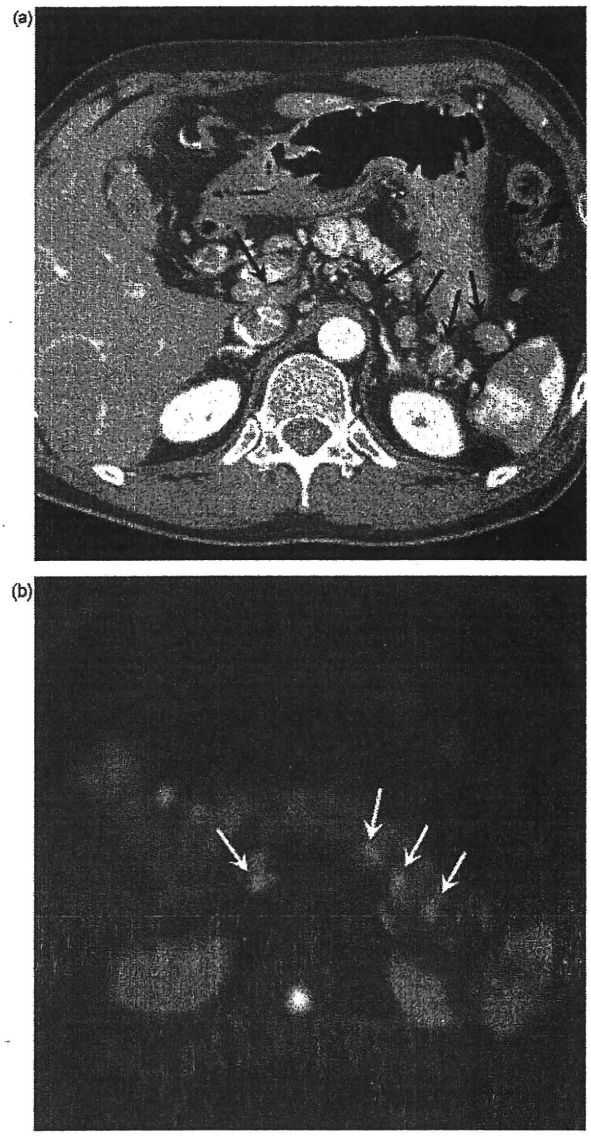

Fig. 7. Peri-pancreatic and para-aortic lymphadenopathy in a 55-year-old man. (a) Contrast-enhanced CT shows multiple peri-pancreatic lymphadenopathy (arrows). (b) On diffusion-weighted images, these lesions are detected as high intensity signals (white arrows).

3.6. Renal lesions

CT or MRI showed renal lesions in 13 of 90 cases (14%), including parenchymal lesions in 10 and hilar lesions in 3 (Fig. 2c) (Table 1). Four renal parenchymal lesions and 1 hilar lesion were diagnosed by biopsies and other 12 cases were clinically diagnosed. All 10 parenchymal lesion cases had multiple bilateral lesions, and 2 had unilateral renal atrophy. Contrast-enhanced CT showed renal parenchymal lesions as slightly enhanced wedge- or node-shaped lesions. Multiphase dynamic contrast-enhanced CT were performed in 5 of 10 patients and revealed that the shapes changed over time and were ill-defined in the delayed phase (Fig. 8) in all cases. Renal lesions were unclear on T1-weighted MR images, but

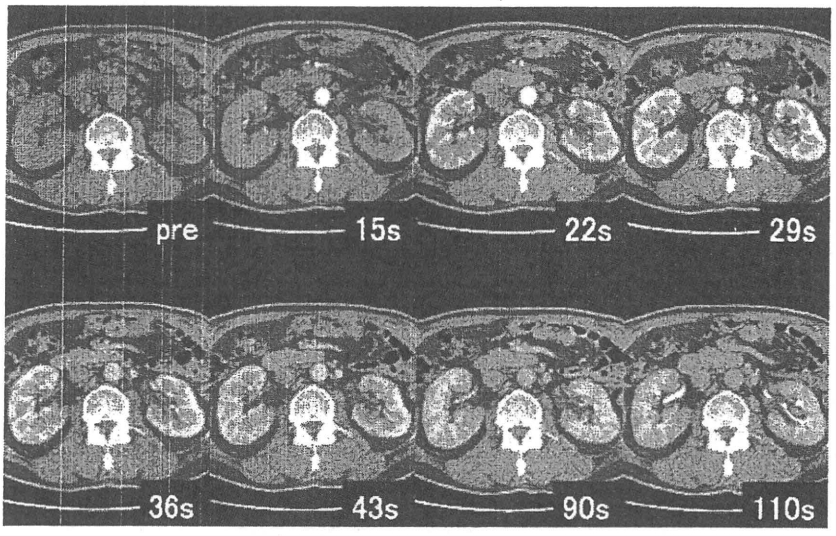

Fig. 8. Renal lesions in a 67-year-old man (same case as in Fig. 1). Multiphase dynamic contrast-enhanced CT shows multiple poorly enhanced lesions in both kidneys, and sequential changes in the lesions over time.

had slightly high intensity on T2-weighted MR images, and high intensity on diffusion-weighted images. These lesions were wedge- or node-shaped on dynamic multiphase T1-weighted images. CT and MRI showed prominent and diffuse renal pelvic wall thickening in renal hilus lesions. Ga-67 scintigraphy showed increase uptake in all renal lesions.

3.7. Retroperitoneal lesions

CT showed retroperitoneal fibrosis in 17 of the 86 cases for which findings were available (20%) (Table 1), including a soft tissue density around the aorta in 11 (Fig. 9a), soft tissue masses around both ureters in 3 (Fig. 9b), paravertebral masses in 2, a pelvic retroperitoneal mass in 1, and increased fat density around the superior mesenteric artery in 1 (Fig. 9c). The biopsy specimens from 3 para-aortic lesion cases and 2 peri-ureteral lesion cases showed abundant IgG4 plasma cell infiltration. A paravertebral mass and pelvic retroperitoneal mass were observed together in the same patient (Fig. 2d, e). Three of 11 cases with para-aortic lesions had aortic aneurysms. One of 3 cases with peri-ureteral lesions had hydronephrosis.

3.8. Other lesions

CT or MRI showed *ligamentum teres* lesions in 2 of the 90 cases (2%) (Table 1). Both lesions were clinically diagnosed and no biopsy was taken. These lesions showed a spindle-shaped soft tissue mass on CT, hypointense mass on T1-weighted image, and hyperintense mass on T2-weighted images (Fig. 10).

Ga-67 scintigraphy exhibited Ga-67 accumulation in the prostate in 8 of 80 cases (10%) (Table 1). Biopsy specimens from two patients showed abundant IgG4-positive plasma cells and lymphocyte infiltration. Other six patients were clinically diagnosed. Diffusion-weighted MRI showed prostatic swelling with high intensity signals (Fig. 11), which mimicked prostate cancer or prostatitis.

4. Discussion

The present study demonstrated some characteristics found in images of various extra-pancreatic lesions associated with AIP. Because they favorably respond to corticosteroid therapy, it is important to differentiate these IgG4-related extra-pancreatic lesions from other diseases that might affect the same organs, including Sjögren's syndrome, sarcoidosis, and primary sclerosing cholangitis. In general, differentiation has previously been based on histological findings and the response to corticosteroid therapy. In this study, we aimed to identify characteristics in images that would be useful for the diagnosis and differentiation of AIP-related lesions with noninvasive imaging.

The major causes of lachrymal and salivary gland swelling include Sjögren's syndrome, Mikulicz disease, or Küttner tumors. Recent reports have shown that high serum IgG4 concentrations and abundant IgG4-bearing plasma cell infiltration were associated with Mikulicz disease and Küttner tumors, but not Sjögren's syndrome [40–42]. In our series, lachrymal and salivary gland lesions responded well to corticosteroid therapy, and thus were similar to those described in Mikulicz disease and Küttner tumors. For this reason, we speculate that the lachrymal and salivary gland lesions associated with AIP may arise from the same or similar systemic conditions as those associated with Mikulicz disease and Küttner tumors.

In our series, 95% of the patients presented with lachrymal or submandibular gland enlargement and only five patients (12.5%) presented with parotid gland enlargement. By contrast, patients with Sjögren's syndrome frequently present with parotid gland enlargement. This difference in the distribution of lesions might be important for the differentiation of AIP-associated lesions and Sjögren's syndrome lesions. In addition, a salt-and-pepper appearance is typically found on the MRIs in Sjögren's syndrome [38]. By contrast, the salivary gland lesions in our series always exhibited homogeneous swelling. This difference in imaging characteristics should be helpful for the differentiation between the two diagnoses. Furthermore, we found that increased Ga-67 uptake by the pancreas and the presence of other extra-pancreatic lesions are indicative of an AIP diagnosis.

Hilar Ga-67 accumulation has been reported in other diseases, including sarcoidosis or primary biliary cirrhosis. Thus, it is necessary to differentiate between these diseases and AIP. Saegusa et al. reported that hilar and pancreatic Ga-67 accumulations are characteristic features of AIP during the active stage of the disease [26].

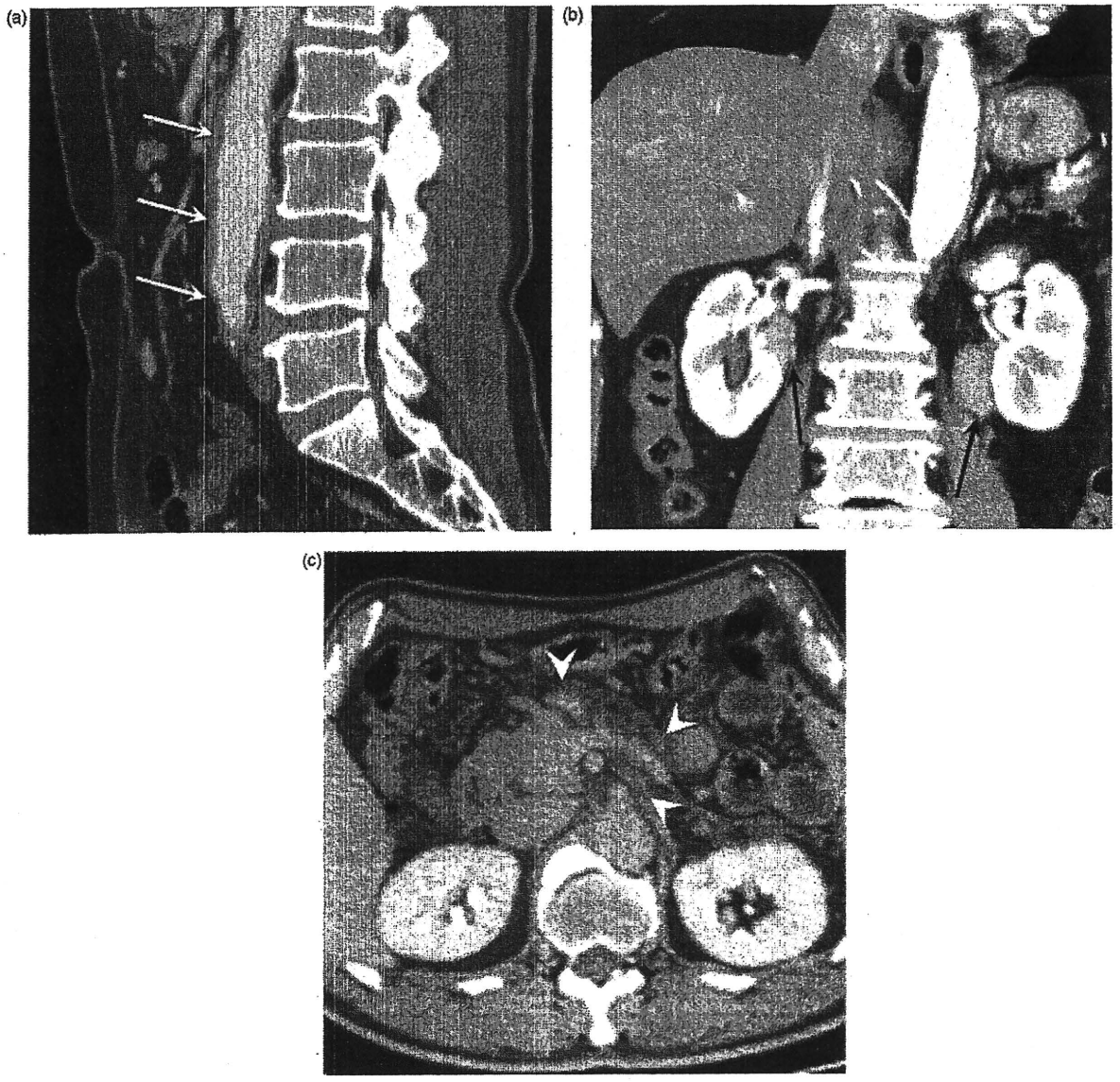

Fig. 9. Retroperitoneal lesions. (a) Sagittal reformation of contrast-enhanced CT shows a soft tissue mass along the aorta (white arrows). (b) Coronal reformation of contrast-enhanced CT shows masses around both ureters (arrows). No hydronephrosis is observed. (c) Axial contrast-enhanced CT shows increased fat density around superior mesenteric artery and splenic vein (white arrow heads).

In our series, almost all patients had Ga-67 accumulation in the pancreas and, concomitantly, in extra-pancreatic lesions, including the lachrymal gland, salivary gland, lung, retroperitoneum and/or prostate. Systemic Ga-67 accumulation was helpful for diagnosing AIP-associated hilar lymphadenopathy. In addition, a normal serum ACE value might be helpful for the exclusion of sarcoidosis.

Radiologically, lung lesions associated with AIP were similar to those indicative of nonspecific inflammatory nodules, chronic bronchitis, chronic bronchiolitis, nonspecific interstitial pneumonia (NSIP), and lymphocytic interstitial pneumonia (LIP). All these lesions had a tendency to spread in the interstitial space of the lung, including the lymphoid channel. At present, we have no clear understanding of the relationship between AIP-related lung lesions and other lung lesions; this remains an issue for future study.

Bile duct abnormality was the most common abdominal finding associated with AIP in the present study, though Shoe et al. reported that retroperitoneal fibrosis was most frequently seen among abdominal lesions in AIP patients [36]. We suspect that differences in the case numbers and study methods were the cause of this disparity. The bile duct wall thickening found in AIP-associated lesions has not been reported in primary sclerosing cholangitis or bile duct carcinoma. In the absence of swelling of the pancreas head, intrahepatic bile duct dilatation was mild, regardless of the bile duct wall thickness. These findings were helpful in differentiating between AIP-associated lesions and those associated with PSC or bile duct carcinoma. In addition, a favorable response to corticosteroid therapy was a distinguishing factor between AIP- and PSC-related lesions, although some sclerosing cholangitis can be

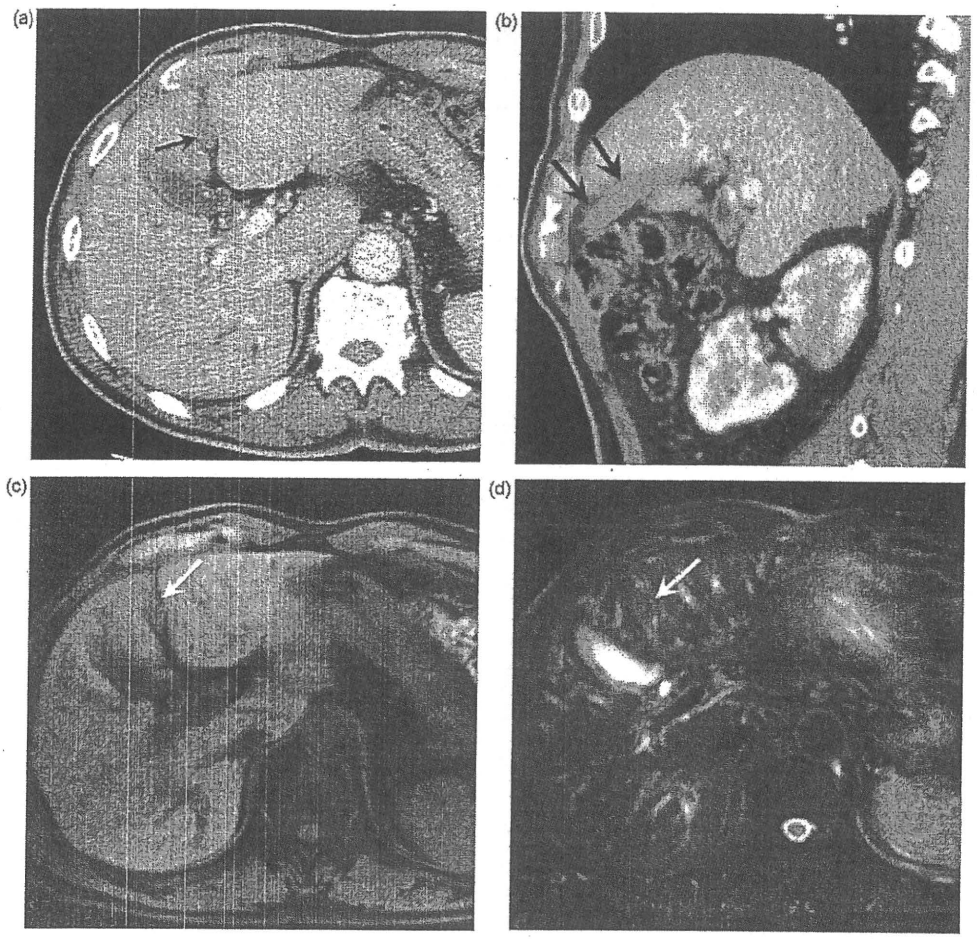

Fig. 10. Lesions in the *ligamentum teres*. (a) Contrast-enhanced CT shows soft tissues mass in the *ligamentum teres* (arrow). (b) Saggital image of contrast-enhanced CT shows the spindle-shape mass along *ligamentum teres* (large arrows). (c–d) MR images show hypointense mass on fat saturated T1-weighted images and hyperintense mass on fat saturated T2-weighted images (white arrows).

cured by steroid therapy [7,17,20,43,44]. However, pancreatic and bile duct lesions had similar pathologies [27,45–47]; thus, when diagnosis with imaging is difficult, a biopsy should be performed. Endoscopic retrograde cholangiopancreatography (ERCP) has also been reported to be useful for differentiating between AIP- and PSC-associated lesions [48].

AIP-associated peri-pancreatic or para-aortic lymphadenopathy is not easily distinguished from inflammatory lymph node swelling and malignant lymphomas. We found that the coexistence of lymphadenopathies and pancreatic lesions is the only distinguishing feature of AIP.

Poorly enhanced multiple wedge-shaped or round lesions associated with AIP are not easily differentiated from those associated with pyelonephritis or infarctions [49,50]. We found graduated enhancement on dynamic contrast-enhanced CTs or MRIs and increased Ga-67 uptake; these characteristics might be specific for AIP-associated renal lesions. Renal hilus lesions are often difficult to differentiate from urothelial tumors, retroperitoneal fibrosis, and lymphomas. Our results suggested that the observation of a combination of pancreatic and extra-pancreatic lesions would be indicative of AIP.

There are only a few reports that describe para-aortic soft tissue masses associated with AIP [12,36,51,52]. Results from those studies were consistent with our findings of a broad homogeneous soft tissue mass along the aorta. This finding should be useful for differentiating AIP from other inflammatory conditions and retroperitoneal tumors. However, the diagnosis is often difficult when a slightly increased density of fat is observed. Kasashima et al. reported that one type of inflammatory abdominal aortic aneurysm was IgG4-related and may be the result of IgG4-related peri-aortitis or retroperitoneal fibrosis [53]. In our series, 3 of 11 patients with para-aortic soft tissue thickening were diagnosed with aortic aneurysms. Hence, IgG4-related para-aortic soft tissue thickening might increase the risk of developing an aortic aneurysm.

This was the first report of AIP-associated *ligamentum teres* lesions. They were rare (2%) but characteristic finding, and both lesions disappeared after corticosteroid therapy. If the Ga-67 scintigraphy shows increased uptake in these lesions, extra-pancreatic lesions associated with AIP can be easily differentiated from other tumors or tumor-like lesions, such as metastatic tumors, leiomyoma, leiomyosarcoma, and extramedullary hematopoiesis because Ga-67 accumulation is very rare in these tumors.

We found prostatic lesions by Ga-67 scintigraphy and diffusion-weighted MRIs. These were often difficult to differentiate from prostate cancer and prostatitis. We found that biopsy was manda-

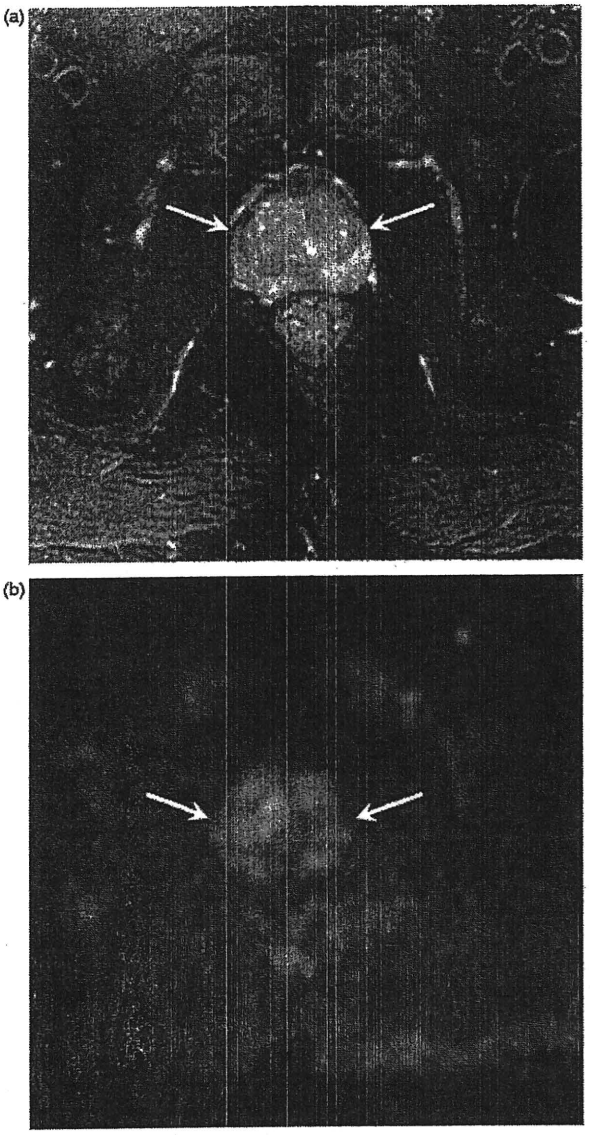

Fig. 11. Prostatic lesions in a 66-year-old man (same case as in Fig. 9a). (a) Axial T2-weighted image with fat saturation shows prostate swelling (white arrows). No mass lesions can be detected. (b) Diffusion-weighted image shows diffuse high intensity signal in the prostate (white arrows).

tory for confirming abundant IgG4-positive plasma cells and lymphocyte infiltration; in addition, a favorable response to corticosteroid therapy was helpful in identifying AIP. To date, a few AIP-associated prostate lesions have been reported, but detailed image findings have not been previously described [54,55].

In this study, we described variable findings of multiple AIP-associated soft tissue masses in the kidney, around the ureter, aorta, paravertebral region, *ligamentum teres*, and orbit. These lesions resembled inflammatory pseudotumors because they frequently contained abundant plasma cell infiltration. Diagnostic imaging played an important role in detecting these lesions, and the characteristic finding of multiple lesions may provide a useful tool for the correct diagnosis of AIP-associated lesions.

AIP and AIP-associated extra-pancreatic lesions are frequently found simultaneously; thus, it is important to examine all other organs when a pancreatic lesion is found. However, these lesions are not always synchronous; thus, successive diagnostic imaging should be mandatory for the detection of newly occurring AIP-associated lesions.

Our study had some limitations, mainly due to using variable models as well as variable scan protocols of CT, MRI and gamma camera because of the length of period reviewed in our retrospective study. Furthermore, all patients were not checked by every image test. Another limitation was that many extra-pancreatic lesions were not histopathologically proven. Therefore, there is a problem that some of the lesions improved by corticosteroid therapy might not be always AIP related extra-pancreatic lesions. Conversely, some of the lesions that were not improved by corticosteroid therapy might include AIP related extra-pancreatic lesions. This problem was not analyzed in this study.

5. Conclusion

AIP is accompanied by various extra-pancreatic lesions and characterized by a variety of image findings. Diagnostic imaging plays an important role in the comprehensive evaluation of these lesions. Radiologists and physicians should keep in mind that multiple lesions may or may not be synchronous under different conditions.

References

[1] Sarles H, Sarles JC, Muratore R, Guien C. Chronic inflammatory sclerosis of the pancreas—an autonomous pancreatic disease? Am J Dig Dis 1961;6:688–98.
[2] Kawaguchi K, Koike M, Tsuruta K, Okamoto A, Tabata I, Fujita N. Lymphoplasmacytic sclerosing pancreatitis with cholangitis: a variant of primary sclerosing cholangitis extensively involving pancreas. Hum Pathol 1991;22:387–95.
[3] Toki F, Kozu T, Oi I, Nakasato T, Suzuki M, Hanyu F. An unusual type of chronic pancreatitis showing diffuse irregular narrowing of the entire main pancreatic duct on ERCP—a report of four cases. Endoscopy 1992;24:640 [abstract].
[4] Wakabayashi T, Motoo Y, Kojima Y, Makino H, Sawabu N. Chronic pancreatitis with diffuse irregular narrowing of the main pancreatic duct. Dig Dis Sci 1998;43:2415–25.
[5] Horiuchi A, Kaneko T, Yamamura N, et al. Autoimmune chronic pancreatitis simulating pancreatic lymphoma. Am J Gastroenterol 1996;91:2607–9.
[6] Horiuchi A, Kawa S, Akamatsu T, et al. Characteristic pancreatic duct appearance in autoimmune chronic pancreatitis: a case report and review of the Japanese literature. Am J Gastroenterol 1998;93:260–3.
[7] Erkelens GW, Vleggaar FP, Lesterhuis W, van Buuren HR, van der Werf SD. Sclerosing pancreato-cholangitis responsive to steroid therapy. Lancet 1999;354:43–4.
[8] Okazaki K, Uchida K, Ohana M, et al. Autoimmune-related pancreatitis is associated with autoantibodies and a Th1/Th2-type cellular immune response. Gastroenterology 2000;118:573–81.
[9] Okazaki K, Chiba T. Autoimmune related pancreatitis. Gut 2002;51:1–4.
[10] Uchida K, Okazaki K, Konishi Y, et al. Clinical analysis of autoimmune-related pancreatitis. Am J Gastroenterol 2000;95:2788–94.
[11] Hamano H, Kawa S, Horiuchi A, et al. High serum IgG4 concentrations in patients with sclerosing pancreatitis. N Engl J Med 2001;344:732–8.
[12] Hamano H, Kawa S, Ochi Y, et al. Hydronephrosis associated with retroperitoneal fibrosis and sclerosing pancreatitis. Lancet 2002;359:1403–4.
[13] Yoshida K, Toki F, Takeuchi T, Watanabe S, Shiratori K, Hayashi N. Chronic pancreatitis caused by an autoimmune abnormality. Proposal of the concept of autoimmune pancreatitis. Dig Dis Sci 1995;40:1561–8.
[14] Ito T, Nakano I, Koyanagi S, et al. Autoimmune pancreatitis as a new clinical entity. Three cases of autoimmune pancreatitis with effective steroid therapy. Dig Dis Sci 1997;42:1458–68.
[15] Kawa S, Ota M, Yoshizawa K, et al. HLA DRB10405-DQB10401 haplotype is associated with autoimmune pancreatitis in the Japanese population. Gastroenterology 2002;122:1264–9.
[16] Horiuchi A, Kawa S, Hamano H, Hayama M, Ota H, Kiyosawa K. ERCP features in 27 patients with autoimmune pancreatitis. Gastrointest Endosc 2002;55:494–9.
[17] Hirano K, Shiratori Y, Komatsu Y, et al. Involvement of the biliary system in autoimmune pancreatitis: a follow-up study. Clin Gastroenterol Hepatol 2003;1:453–564.
[18] Kamisawa T, Funata N, Hayashi Y, et al. Close relationship between autoimmune pancreatitis and multifocal fibrosclerosis. Gut 2003;52:683–7.
[19] Nakazawa T, Ohara H, Yamada T, et al. Atypical primary sclerosing cholangitis cases associated with unusual pancreatitis. Hepatogastroenterology 2001;48:625–30.

[20] Horiuchi A, Kawa S, Hamano H, Ochi Y, Kiyosawa K. Sclerosing pancreatocholangitis responsive to corticosteroid therapy: report of 2 case reports and review. Gastrointest Endosc 2001;53:518–22.
[21] Notohara K, Burgart LJ, Yadav D, Chari S, Smyrk TC. Idiopathic chronic pancreatitis with periductal lymphoplasmacytic infiltration: clinicopathologic features of 35 cases. Am J Surg Pathol 2003;27:1119–27.
[22] Hardacre JM, Iacobuzio-Donahue CA, Sohn TA, et al. Results of pancreaticoduodenectomy for lymphoplasmacytic sclerosing pancreatitis. Ann Surg 2003;237:853–9.
[23] Kamisawa T, Egawa N, Nakajima H, Tsuruta K, Okamoto A, Kamata N. Clinical difficulties in the differentiation of autoimmune pancreatitis and pancreatic carcinoma. Am J Gastroenterol 2003;98:2694–9.
[24] Nakano S, Takeda I, Kitamura K, Watahiki H, Iinuma Y, Takenaka M. Vanishing tumor of the abdomen in patient with Sjögren's syndrome. Am J Dig Dis 1978;23(Suppl.):75S–9S.
[25] Komatsu K, Hamano H, Ochi Y, et al. High prevalence of hypothyroidism in patients with autoimmune pancreatitis. Dig Dis Sci 2005;50:1052–7.
[26] Saegusa H, Momose M, Kawa S, et al. Hilar and pancreatic gallium-67 accumulation is characteristic feature of autoimmune pancreatitis. Pancreas 2003;27:20–5.
[27] Uchida K, Okazaki K, Asada M, et al. Case of chronic pancreatitis involving an autoimmune mechanism that extended to retroperitoneal fibrosis. Pancreas 2003;26:92–4.
[28] Fukukura Y, Fujiyoshi F, Nakamura F, Hamada H, Nakajo M. Autoimmune pancreatitis associated with idiopathic retroperitoneal fibrosis. AJR Am J Roentgenol 2003;181:993–5.
[29] Kamisawa T, Nakajima H, Egawa N, Funata N, Tsuruta K, Okamoto A. IgG4-related sclerosing disease incorporating sclerosing pancreatitis, cholangitis, sialadenitis and retroperitoneal fibrosis with lymphadenopathy. Pancreatology 2006;6:132–7.
[30] Taniguchi T, Ko M, Seko S, et al. Interstitial pneumonia associated with autoimmune pancreatitis. Gut 2004;53:770.
[31] Hirano K, Kawabe T, Komatsu Y, et al. High-rate pulmonary involvement in autoimmune pancreatitis. Intern Med J 2006;36:58–66.
[32] Takeda S, Haratake J, Kasai T, Takaeda C, Takazakura E. IgG4-associated idiopathic tubulointerstitial nephritis complicating autoimmune pancreatitis. Nephrol Dial Transplant 2004;19:474–6.
[33] Uchiyama-Tanaka Y, Mori Y, Kimura T, et al. Acute tubulointerstitial nephritis associated with autoimmune-related pancreatitis. Am J Kidney Dis 2004;43:e18–25.
[34] Ohara H, Nakazawa T, Sano H, et al. Systemic extrapancreatic lesions associated with autoimmune pancreatitis. Pancreas 2005;31:232–7.
[35] Hamano H, Arakura N, Muraki T, Ozaki Y, Kiyosawa K, Kawa S. Prevalence and distribution of extrapancreatic lesions complicating autoimmune pancreatitis. J Gastroenterol 2006;41:1197–205.
[36] Sohn JH, Byun JH, Yoon SE, et al. Abdominal extrapancreatic lesions associated with autoimmune panvcreatitis: radiological findings and changes after therapy. Eur J Radiol 2008;67:497–507.
[37] Members of the Criteria Committee for Autoimmune Pancreatitis of the Japan Pancreas Society. Diagnostic criteria for autoimmune pancreatitis by the Japan Pancreas Society (in Japanese with English abstract). Suizo (J Jpn Pancreas Soc) 2002;17:585–7.
[38] Okazaki K, Kawa S, Kamisawa T, et al. Clinical diagnostic criteria of autoimmune pancreatitis—revised proposal. J Gastroenterol 2006;41:626–31.
[39] Takashima S, Takeuchi N, Morimoto S, et al. MR imaging of Sjögren syndrome: correlation with sialography and pathology. J Comput Assist Tomogr 1991;15:393–400.
[40] Yamamoto M, Ohara M, Suzuki C, et al. Elevated IgG4 concentrations in serum of patients with Mikulicz's disease. Scand J Rheumatol 2004;33:432–3.
[41] Yamamoto M, Takahashi H, Sugai S, Imai K. Clinical and pathological characteristics of Mikulicz's disease (IgG4-related plasmacytic exocrinopathy). Autoimmun Rev 2006;4:195–200.
[42] Kitagawa S, Zen Y, Harada K, et al. Abundant IgG4-positive plasma cell infiltration characterizes chronic sclerosing sialadenitis (Kuttner's tumor). Am J Surg Pathol 2005;29:783–91.
[43] Eerens I, Vanbeckevoort D, Vansteenbergen W, Van Hoe L. Autoimmune pancreatitis associated with primary sclerosing cholangitis: MR imaging findings. Eur Radiol 2001;11:1401–4.
[44] Kuroiwa T, Suda T, Takahashi T, et al. Bile duct involvement in a case of autoimmune pancreatitis successfully treated with an oral steroid. Dig Dis Sci 2002;47:1810–6.
[45] Zen Y, Harada K, Sasaki M, et al. IgG4-related sclerosing cholangitis with and without hepatic inflammatory pseudotumor, and sclerosing pancreatitis-associated sclerosing cholangitis: do they belong to a spectrum of sclerosing pancreatitis? Am J Surg Pathol 2004;28:1193–203.
[46] Uehara T, Hamano H, Kawa S, Sano K, Honda T, Ota H. Distinct clinicopathological entity 'autoimmune pancreatitis-associated sclerosing cholangitis'. Pathol Int 2005;55:405–11.
[47] Hamano H, Kawa S, Uehara T, et al. Immunoglobulin G4-related lymphoplasmacytic sclerosing cholangitis that mimics infiltrating hilar cholangiocarcinoma: part of a spectrum of autoimmune pancreatitis? Gastrointest Endosc 2005;62:152–7.
[48] Nakazawa T, Ohara H, Sano H, et al. Cholangiography can discriminate sclerosing cholangitis with autoimmune pancreatitis from primary sclerosing cholangitis. Gastrointest Endosc 2004;60:937–44.
[49] Takahashi N, Kawashima A, Fletcher JG, Chari ST. Renal involvement in patients with autoimmune pancreatitis: CT and MR imaging findings. Radiology 2007;242:791–801.
[50] Saeki T, Nishi S, Ito T, et al. Renal lesions in IgG4-related systemic disease. Intern Med 2007;46:1365–71.
[51] Zen Y, Sawazaki A, Miyayama SK, Tanaka N, Nakanuma Y. A case of retroperitoneal and mediastinal fibrosis exhibiting elevated levels of IgG4 in the absence of sclerosing pancreatitis (autoimmune pancreatitis). Hum Pathol 2006;37:239–43.
[52] Kamisawa T, Chen PY, Tu Y, Nakajima H, Egawa N. Autoimmune pancreatitis metachronously associated with retroperitoneal fibrosis with IgG4-positive plasma cell infiltration. World J Gastroenterol 2006;12:2955–7.
[53] Kasashima S, Zen Y, Kawashima A, et al. Inflammatory abdominal aortic aneurysm: close relationship to IgG4-related periaortitis. Am J Surg Pathol 2008;32:197–204.
[54] Yoshimura Y, Takeda S, Ieki Y, Takazakura E, Koizumi H, Takagawa K. IgG4-associated prostatitis complicating autoimmune pancreatitis. Intern Med 2006;45:897–901.
[55] Hamed G, Tsushima K, Yasuo M, et al. Inflammatory lesions of the lung, submandibular gland, bile duct and prostate in a patient with IgG4-associated multifocal systemic fibrosclerosis. Respirology 2007;12:455–7.

Chronic Gastritis in the Setting of Autoimmune Pancreatitis

Takeshi Uehara, PhD, MD, Hideaki Hamano, PhD, MD,† Shigeyuki Kawa, PhD, MD,‡ Kenji Sano, PhD, MD,* Keiko Oki,§ Yukihiro Kobayashi, PhD,§ Tadanobu Nagaya, MD,† Taiji Akamatsu, PhD, MD,† Masahiro Kurozumi, MD,‖ Yasunori Fujinaga, PhD, MD,‖ Eiji Tanaka, PhD, MD,† Takayuki Honda, PhD, MD,* and Hiroyoshi Ota, PhD, MD,*¶*

Abstract: Autoimmune pancreatitis (AIP) is a recently recognized disease entity. In some patients, this disease is associated with other inflammatory diseases. In this study, we aimed to elucidate the pathologic characteristics of AIP-associated gastritis (AIP-G). We evaluated and compared the pathologic findings and immunohistochemical expressions of immunoglobulin G (IgG)4 and IgG in gastric biopsy specimens from 13 AIP-G patients with those from patients of 2 control groups. We divided the AIP-G patients who did not receive steroid therapy [AIP-G-ST(−)] into the following 2 groups: without *Helicobacter pylori* (HP) infection [AIP-G-HP(−)] and with HP infection [AIP-G-HP(+)]. The control groups comprised 19 patients who were diagnosed with chronic active gastritis associated with HP infection and 7 patients with nonsteroidal anti-inflammatory drug-induced gastritis. We classified the findings for the gastric mucosa into those for the upper and the lower lamina propria. The characteristic finding of AIP-G groups was diffusely lymphoplasmacytic infiltration in the lamina propria. The IgG4-positive plasma cell/IgG-positive plasma cell ratios (IgG4/IgG ratios) in both the upper and lower lamina propria in the AIP-G-ST(−) groups were predominantly higher than the corresponding values in the other groups. In the AIP-G-ST(−) groups, the IgG4/IgG ratio in the lower lamina propria was predominantly higher than that in the upper lamina propria, irrespective of the HP status. In conclusion, diffuse lymphoplasmacytic infiltration in the lamina propria and increased IgG4/IgG ratio in the gastric mucosa (notably in the lower lamina propria) may be the characteristic findings of AIP-G.

Key Words: autoimmune pancreatitis, IgG4, gastritis

(*Am J Surg Pathol* 2010;34:1241–1249)

From the Departments of *Laboratory Medicine; ‖Radiology; ¶Biomedical Laboratory Medicine; †Second Department of Internal Medicine, Shinshu University School of Medicine; ‡Center for Health, Safety and Environmental Management, Shinshu University; and §Department of Laboratory Medicine, Shinshu University Hospital, Matsumoto, Japan.

Correspondence: Takeshi Uehara, PhD, MD, Department of Laboratory Medicine, Shinshu University School of Medicine, Asahi 3-1-1, Matsumoto 390-8621, Japan (e-mail: tuehara@shinshu-u.ac.jp).

The relationship between immunoglobulin G (IgG)4 and sclerosing disease with regard to autoimmune pancreatitis (AIP) was first reported in 2001.[6] AIP, also known as lymphoplasmacytic sclerosing pancreatitis, is a unique form of pancreatitis characterized by the following findings: (1) irregular narrowing of the main pancreatic duct because of fibrosis and lymphoplasmacytic infiltration and an increased number of IgG4-positive plasma cells and eosinophils in the pancreas; (2) hypergammaglobulinemia with a predominant increase in the IgG4 levels; and (3) alleviation of symptoms after steroid therapy.[9,14,32] AIP is now recognized as a distinct entity worldwide.[15,17,22]

AIP has also been reported to be associated with various diseases in organs other than those in the pancreaticobiliary system[2,10,17,25]; these diseases include chronic sialadenitis, retroperitoneal inflammation,[7,11,27] lymphadenopathy of the intra-abdominal, hilar, or mediastinal lymph nodes,[18] interstitial pneumonia,[8,24] pulmonary inflammatory pseudotumor,[28,30] hepatic inflammatory pseudotumor,[12,19,29] inflammatory abdominal aortic aneurysm,[13] prostatitis,[26] and tubulointerstitial nephritis.[23,24] Further, Kamisawa et al[10] have proposed that AIP is the pancreatic lesion involved in a new clinicopathologic entity, namely, IgG4-related sclerosing disease.

Many cases of chronic active gastritis associated with *Helicobacter pylori* (HP) infection (CAG) have been reported in Japan.[5] Few cases of gastritis not associated with HP infection have also been reported.[16] Recently, Shinji et al[21] found that the incidence of IgG4-positive plasma cells in gastric biopsy specimens from patients with AIP was significantly higher than that in specimens from patients with CAG. However, the distribution of IgG4-positive plasma cells and the characteristic histopathologic findings of AIP-associated gastritis (AIP-G) have not been reported. To elucidate the clinicopathologic characteristics of AIP-G, we evaluated the clinicopathologic findings of patients with AIP-G and compared the immunohistochemical expression of IgG4 in the AIP-G patients with that in the control groups, which included patients with abdominal distress.

MATERIALS AND METHODS

Patients and Materials

Between 2002 and 2009, we analyzed 13 AIP-G (Table 1) and 26 control patients at the Shinshu University

TABLE 1. Clinical Features of Autoimmune Pancreatitis-associated Gastritis

Case No.	Age (y)	Sex	Pathologic Diagnosis	Biopsy Area	HP	Serum IgG4 (mg/dL)*	Endoscopic Finding	Symptom
1	79	M	CG	FA	Negative	1950	Redness	EG
2	53	F	CG	PA, FA	Negative	227	NP	NP
3	59	M	CG	PA, FA	Negative	965	Erosion	NP
4	55	M	CG	FA	Negative	2970	NP	NP
5	76	F	CG	PA	Negative	420	Erosion	NP
6	56	M	CAG	FA	Positive	156	NP	NP
7	62	M	CAG	PA, FA	Positive	305	Atrophy	NV
8	60	M	CAG	FA	Positive	1240	NP	NP
9	62	M	CAG	PA, FA	Positive	825	NP	NP
10	78	M	CAG	FA	Positive	541	NP	NP
11	76	M	CAG	PA, FA	Positive	698	Redness	NP
12	56	M	CAG	PA, FA	Positive	265	NP	EG
13	67	M	CAG	PA, FA	Positive	500	NP	EG

*Normal value: IgG4, < 70 mg/dL (cut-off value, 135 mg/dL).

CAG indicates chronic active gastritis with HP infection; CG, chronic gastritis; EG, epigastralgia; F, female; FA, fundic area; HP, *Helicobacter pylori*; IgG, immunoglobulin G; M, male; NP, nothing particular; NV, nausea and vomiting; PA, pyloric area.

Hospital. Of the 13 API-G patients, 9 had no symptoms, 3 had epigastralgia (patients 1, 12, and 13), and 1 had nausea and vomiting (patient 7).

All the patients with AIP-G showed the following characteristic findings of AIP: (1) irregular narrowing of the main pancreatic duct, (2) sonolucent swelling of the pancreas, (3) hypergammaglobulinemia, and (4) high serum IgG4 level (cut-off value, 135 mg/dL). All the patients with AIP-G underwent enhanced abdominal computed tomography (CT) and Gallium (Ga)-67 citrate scintigraphy for the pancreatic lesions. One patient (patient 1) underwent pancreatoduodenectomy. The patient was diagnosed as having AIP, because of the presence of lymphoplasmacytic sclerosing pancreatitis without neutrophil infiltration and cancer. The other AIP-G patients did not undergo any operation for the pancreatic lesions and biopsy for suspected pancreatic cancer.

The histologic specimens obtained from the 13 AIP-G patients included biopsy specimens. The stomach biopsy specimens obtained from 7 patients (patients 2, 3, 7, 9, 11, 12, and 13) included specimens from both the fundic and pyloric areas, those from the other 5 patients (patients 1, 4, 6, 8, and 10) included specimens only from the fundic area, and those from the remaining 1 patient (patient 5) included specimens only from the pyloric area. In 4 patients (patients 2, 3, 11, and 13), the specimens were obtained from 6 biopsy points. HP infection was detected only in the specimens from 8 of the 13 patients (patients 6, 7, 8, 9, 10, 11, 12, and 13). Of the 8 AIP-G patients who had HP infection, 2 developed the infection after steroid therapy (patient 12 and 13). Patient 1 was receiving proton pump inhibitor therapy, although he was free of HP infection. First, we divided the AIP-G patients into the following 2 groups: steroid nontreated group [AIP-G-ST(−)] and steroid treated group [AIP-G-ST(+)]. We further divided the AIP-G-ST(−) patients into the following 2 groups: without HP infection [AIP-G-HP(−)] and with HP infection [AIP-G-HP(+)].

The control groups were divided into the following 2 groups: CAG and nonsteroidal anti-inflammatory drug (NSAID)-induced gastritis (NSAID-G). The CAG group comprised 19 patients who were clinically diagnosed with chronic active gastritis caused by HP infection. The NSAID-G group comprised 7 patients with no HP infection. None of the patients in the control groups showed the characteristic findings of AIP.

Histopathology and Immunohistochemistry

All the specimens from the 39 patients were fixed in 20% formaldehyde and embedded in paraffin. Next, 4-μm-thick serial sections were cut from these blocks and stained with hematoxylin-eosin (HE). The sections were treated with rabbit monoclonal antibodies against human IgG (Dako, Glostrup, Denmark; dilution, 1:5000) and affinity-purified sheep polyclonal antibody against human IgG4 (The Binding Site, Birmingham, UK; dilution, 1:50) by using the avidin-biotin immunoperoxidase method. The number of immunohistochemically identified IgG4-positive plasma cells and IgG-positive plasma cells in 10 randomly selected 10000-μm^2-wide areas of the gastric mucosa specimens of the upper and lower lamina propria were counted. The fundic and pyloric mucosae were used for the assessments. The IgG4-positive plasma cell/IgG-positive plasma cell ratio (IgG4/IgG ratio) of the AIP-G group was compared with those of the control groups.

The number of mononuclear cells in the gastric mucosa in 10 randomly selected 10000-μm^2-wide areas of each specimen was also counted. We compared the number of mononuclear cells in the AIP-G group with those in the control group.

Mucosal neutrophilic inflammation, intestinal metaplasia, and glandular atrophy were separately graded as none (0), mild (1+), moderate (2+), or marked (3+), in accordance with the schematic diagrams provided in the Update Sydney System.[3] Eosinophil infiltration was assessed by 2 pathologists (T.U. and H.O.) and graded as

follows: absent or minimal (0), mild (1+), moderate (2+), and severe (3+).

The data are expressed as the median (25th to 75th percentile).

Comparisons were made using the Mann-Whitney *U* test. Differences were considered statistically significant when the *P* value was less than 0.05.

This study was approved by the Ethics Committee of Shinshu University, Japan.

RESULTS

Clinical Findings

Gastric biopsies revealed that, of the 13 patients with AIP-G, 5 had chronic gastritis and 8 had chronic active gastritis. An endoscopic examination revealed that 2 patients had redness, 2 patients had erosion, 1 patient had atrophy, and 8 patients had no abnormal findings. In patient 6, an enhanced abdominal CT image showed thickening of the stomach wall (Fig. 1A), and Ga-67 citrate scintigraphy revealed accumulation of radioactive material on the stomach wall, which was consistent with the findings of the CT analysis (Fig. 1B). Ga-67 citrate scintigraphy did not reveal such accumulations on the stomach walls of other AIP-G patients.

The serum IgG4 levels were not measured in the 26 patients in the control group because there was no evidence of AIP in these patients.

Histologic Findings

We have summarized the histologic characteristics of the AIP-G patients in Tables 2 to 5. Some degree of diffuse lymphoplasmacytic inflammation was observed in the fundic and the pyloric mucosae of all the AIP-G patients (Figs. 2A, B).

In the AIP-G-ST(−) groups, in the fundic mucosa, the number of mononuclear cell infiltrates in the upper lamina propria was not significantly different from that in the lower lamina propria. The number of mononuclear cell infiltrates in the upper lamina propria in the AIP-G-HP(+) group was significantly higher than those in the AIP-G-HP(−) and NSAID-G groups. However, the number of mononuclear cell infiltrates in the upper lamina propria in the AIP-G-HP(−) groups was significantly lower than that in the CAG group. The number of mononuclear cell infiltrates in the lower lamina propria in the AIP-G-ST(−) groups was significantly higher than those in the CAG and NSAID-G groups.

In the AIP-G-ST(−) groups, in the pyloric mucosa, the number of mononuclear cell infiltrates in the upper lamina propria was not significantly different from that in the lower lamina propria. The number of mononuclear cell infiltrates in the upper lamina propria in the AIP-G-HP(+) group was significantly higher than those in the AIP-G-HP(−) and NSAID-G groups. However, the number of mononuclear cell infiltrates in the upper lamina propria in the AIP-G-HP(−) group was significantly lower than that in the CAG group. The number of mononuclear cell infiltrates in the lower lamina propria in the AIP-G-HP(−) groups was higher than that in the NSAID-G group. Further, the number of mononuclear cell infiltrations in the lower lamina propria in the AIP-G-HP(+) group was significantly higher than that in the NSAID-G group.

In the AIP-G-ST(−) groups, the number of mononuclear cell infiltrates in the upper and lower lamina

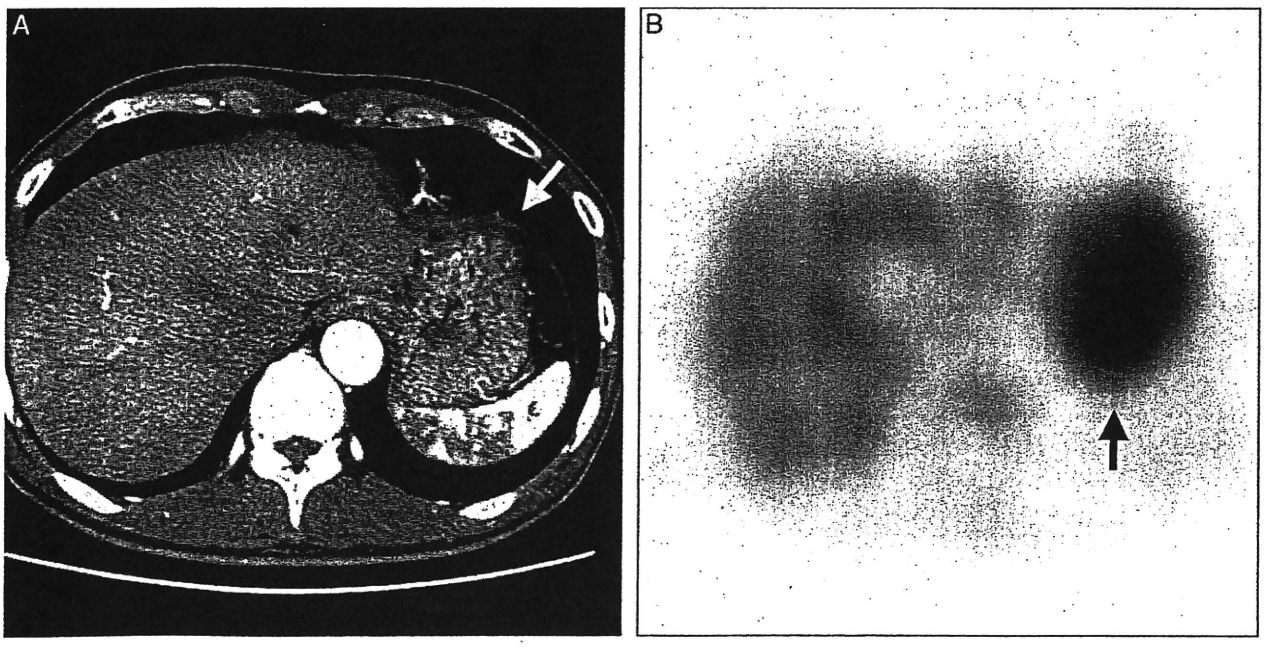

FIGURE 1. A, Enhanced abdominal CT scan shows thickening of the stomach wall (arrow). B, Gallium-67 citrate scintigraphy revealed accumulation of radioactive material on the stomach wall (arrow), which was consistent with the findings of the CT analysis. CT indicates computed tomography.

TABLE 2. Histologic Findings of the Fundic Mucosa From Patients With AIP-G-HP(−), AIP-G-HP(+), CAG, and NSAID-G

	Mono			IgG4/IgG						
	Upper	Lower	*P*	Upper	Lower	*P*	Eosino	Neutro	IM	Atrophy
AIP-G-HP(−) (n = 4)	14.50 (12.00-17.85)	26.55 (11.20-39.30)	0.3865	0.1 (0.05-0.27)	0.76 (0.43-0.82)	0.0433	2 (2-2)	0 (0-0)	0 (0-1.0)	0.5 (0-1.5)
AIP-G-HP(+) (n = 6)	38.75 (29.70-43.70)	33.10 (28.50-37.50)	0.4233	0.1 (0.03-0.19)	0.34 (0.17-0.51)	0.0547	2 (2-3)	1 (1-2)	0 (0-0)	1 (1-1)
CAG (n = 19)	29.20 (18.75-38.58)	4.40 (3.13-5.35)	< 0.0001	0 (0-0.11)	0 (0-0)	0.4221	1 (1-1)	2 (1-2)	0 (0-0)	1 (0.25-1)
NSAID-G (n = 7)	6.50 (4.33-13.45)	0.40 (0.23-2.45)	0.0022	0 (0-0.01)	0 (0-0)	0.7494	0 (0-0)	0 (0-0.75)	0 (0-0)	0 (0-0)
P	0.019*	0.0082†		0.0082†	0.0140†		0.0082†	0.0105*	NS	0.0027‡
	0.0034‡	0.0027‡		0.0184‡	0.010‡		0.0034‡	0.0152‡		
	0.0074§	0.0058§			0.0035§		0.0231§	0.0021§		
		0.0003‖			0.0012‖		0.0186‖			

Data are expressed as the median (25th to 75th percentile).
*AIP-G-HP(–) versus AIP-G-HP(+).
§AIP-G-HP(–) versus CAG.
†AIP-G-HP(–) versus NSAID-G.
‖AIP-G-HP(+) versus CAG.
‡AIP-G-HP(+) versus NSAID-G.
AIP-G indicates autoimmune pancreatitis-associated gastritis; AIP-G-HP(−), AIP-G without steroid therapy and HP infection; AIP-G-HP(+), AIP-G without steroid therapy and with HP infection; CAG, chronic active gastritis with HP infection; Eosino, eosinophil infiltration; HP, *Helicobacter pylori*; IgG, immunoglobulin G; IgG4/IgG, IgG4-positive plasma cells/IgG-positive plasma cells ratio; IM, intestinal metaplasia; Lower, in the lower lamina propria; Mono, number of mononuclear cells; Neutro, neutrophil infiltration; NS, not significant; NSAID-G, nonsteroidal anti-inflammatory drug-induced gastritis; Upper, in the upper lamina propria.

TABLE 3. Histologic Findings of Pyloric Mucosa From Patients With AIP-G-HP(−), AIP-G-HP(+), CAG, and NSAID-G

	Mono			IgG4/IgG						
	Upper	Lower	*P*	Upper	Lower	*P*	Eosino	Neutro	IM	Atrophy
AIP-G-HP(–) (n = 3)	20.10 (16.20-21.60)	22.50 (20.80-34.50)	0.5127	0.17 (0.10-0.25)	0.37 (0.33-0.66)	0.0495	2 (2-2.75)	0 (0-0)	1 (0.25-1)	1 (1-1)
AIP-G-HP(+) (n = 3)	46.30 (43.83-73.15)	22.80 (21.30-38.95)	0.1266	0.06 (0.04-0.12)	0.22 (0.18-0.23)	0.0495	2 (2-2)	2 (2-2)	0 (0-0.75)	0 (0-0.75)
CAG (n = 19)	45.00 (38.78-71.48)	22.70 (15.15-29.85)	< 0.0001	0 (0-0.02)	0 (0-0.03)	0.9651	1 (1-1)	2 (1-2)	1 (0-2)	2 (2-3)
NSAIDs-G (n = 7)	6.50 (5.38-21.65)	4.60 (2.58-15.10)	0.2774	0 (0-0.02)	0 (0-0)	0.3711	0 (0-0)	0 (0-0.0)	0 (0-0.75)	0 (0-1)
P	0.0495*	0.0167†		0.0167‡	0.0495*		0.0167‡	0.0495*	NS	0.0495*
	0.0167†			0.0167†	0.0304‡		0.0167†	0.0167†		0.0304†
	0.0064§			0.0064§	0.0064§		0.0147§	0.0064§		0.0313§
				0.0064‖	0.0129‖		0.0217‖			

Data are expressed as the median (25th to 75th percentile).
*AIP-G-HP(–) versus AIP-G-HP(+).
§AIP-G-HP(–) versus CAG.
‡AIP-G-HP(–) versus NSAID-G.
‖AIP-G-HP(+) versus CAG.
†AIP-G-HP(+) versus NSAID-G.
AIP-G indicates autoimmune pancreatitis-associated gastritis; AIP-G-HP(−), AIP-G without steroid therapy and HP infection; AIP-G-HP(+), AIP-G without steroid therapy and with HP infection; CAG, chronic active gastritis with HP infection; Eosino, eosinophil infiltration; HP, *Helicobacter pylori*; IgG, immunoglobulin G; IgG4/IgG, IgG4-positive plasma cells/IgG-positive plasma cells ratio; IM, intestinal metaplasia; Lower, in the lower lamina propria; Mono, number of mononuclear cells; Neutro, neutrophil infiltration; NS, not significant; NSAID-G, nonsteroidal anti-inflammatory drug-induced gastritis; Upper, in the upper lamina propria.

TABLE 4. Comparison of Histologic Features Between the Fundic and Pyloric Mucosa in AIP-G-HP(−) Patients

	Fundic Mucosa (n = 4)	Pyloric Mucosa (n = 3)	*P*
Mono (upper)	14.50 (12.00-17.85)	20.10 (16.20-21.60)	0.1573
Mono (lower)	26.55 (11.20-39.30)	22.50 (20.80-34.50)	0.7237
IgG4/IgG (upper)	0.1 (0.05-0.27)	0.17 (0.10-0.25)	0.4795
IgG4/IgG (lower)	0.76 (0.43-0.82)	0.37 (0.33-0.66)	0.4795
Eosino	2 (2-2)	2 (2-2.75)	0.4795
Neutro	0 (0-0)	0 (0-0)	> 0.9999
IM	0 (0-1.0)	1 (0.25-1)	0.5959
Atrophy	0.5 (0-1.5)	1 (1-1)	0.5959

Data are expressed as the median (25th to 75th percentile).

AIP-G indicates autoimmune pancreatitis-associated gastritis; AIP-G-HP(−), AIP-G without steroid therapy and *Helicobacter pylori* infection; Eosino, eosinophil infiltration; IgG, immunoglobulin G; IgG4/IgG, IgG4-positive plasma cells/IgG-positive plasma cells ratio; IM, intestinal metaplasia; Lower, in the lower lamina propria; Mono, number of mononuclear cells; Neutro, neutrophil infiltration; Upper, in the upper lamina propria.

propria were not significantly different between the fundic and the pyloric mucosa. In the specimens obtained from 6 biopsy points in 3 patients of the AIP-G-ST(−) group, the distribution of the number of mononuclear cell infiltrates in every case was approximately uniform in the fundic and the pyloric mucosa.

In the AIP-G-ST(+) group, the number of mononuclear cell infiltrates in the fundic mucosa were 12.7 and 10.4 in the upper lamina propria, and 7.0 and 9.1 in the lower lamina propria; and that in the pyloric mucosa were 25.2 and 10.5 in the upper lamina propria, and 16.2 and 3.2 in the lower lamina propria. In the fundic and the pyloric mucosa, the number of mononuclear cell infiltrates in the upper lamina propria was higher than that in the lower lamina propria. In the specimens obtained from 6 biopsy points of 1 patient of the AIP-G-ST(+) group, the distribution of the number of mononuclear cell infiltrates was approximately uniform in the fundic and the pyloric mucosa.

All the AIP-G patients showed mild-to-severe eosinophil infiltration in the fundic mucosa (Fig. 2B). Among the 12 patients with AIP-G, 10 showed mild-to-moderate atrophy and 8 showed mild-to-moderate neutrophilic inflammation; however, none of the patients in the AIP-G-HP(−) group showed neutrophilic inflammation. Moderate intestinal metaplasia was observed in 1 patient in each of the AIP-G-HP(−), AIP-G-HP(+), and AIP-G-ST(+) groups. Patient 6 showed severe fibrosis in the lower lamina propria (Figs. 3A, B). Eosinophil infiltrates in the AIP-G-ST(−) groups were significantly higher than those in the CAG and NSAID-G groups. The number of neutrophil infiltrates in the AIP-G-HP(−) group was significantly lower than those in the AIP-G-HP(+) and CAG groups. The number of neutrophil infiltrates and the degree of atrophy in the AIP-G-HP(+) group were significantly higher than those in the NSAID-G group.

All the AIP-G patients showed moderate-to-severe eosinophil infiltration and mild-to-severe atrophy in the pyloric mucosa. Among the patients in the AIP-G-ST(−) groups, 3 showed mild metaplasia and moderate neutrophilic inflammation; however, none of the AIP-G-HP(−) group patients showed neutrophilic inflammation. Eosinophil infiltrates in the AIP-G-ST(−) groups were significantly higher than those in the CAG and NSAID-G groups. The number of neutrophil infiltrates in the AIP-G-HP(−) group was significantly lower than those in the AIP-G-HP(+) and CAG groups. The number of neutrophil infiltrates in the AIP-G-HP(+) group was significantly higher than that in the NSAID-G group. The degree of atrophy in the AIP-G-HP(−) group was significantly lower than those in the AIP-G-HP(+) and CAG groups. The degree of atrophy in the AIP-G-HP(+) group was significantly higher than that in the NSAID-G group.

In the AIP-G-ST(−) groups, there was no significant difference in the number of eosinophil and neutrophil infiltrates, intestinal metaplasia, and atrophy between the fundic and pyloric mucosa. In the specimen obtained from 6 biopsy points in 3 patients of the AIP-G-ST(−) group, the distribution of inflammation in every case was approximately uniform in the fundic and pyloric mucosa.

In the AIP-G-ST(+) group, the number of eosinophil and neutrophil infiltrates, intestinal metaplasia, and atrophy in the fundic mucosa were mild, moderate, none and moderate, and mild and moderate, respectively. In that group, the number of eosinophil and neutrophil

TABLE 5. Comparison of Histologic Features Between the Fundic and Pyloric Mucosa in AIP-G-HP(+) Patients

	Fundic Mucosa (n = 6)	Pyloric Mucosa (n = 3)	*P*
Mono (upper)	38.75 (29.70-43.70)	46.30 (43.825-73.150)	0.1213
Mono (lower)	33.10 (28.50-37.50)	22.80 (21.30-38.95)	0.6056
IgG4/IgG (upper)	0.1 (0.03-0.19)	0.06 (0.04-0.12)	0.7237
IgG4/IgG (lower)	0.34 (0.17-0.51)	0.22 (0.18-0.23)	0.8597
Eosino	2 (2-3)	2 (2-2)	0.6985
Neutro	1 (1-2)	2 (2-2)	0.1213
IM	0 (0-0)	0 (0-0.75)	0.7963
Atrophy	1 (1-1)	2 (2-2.75)	0.0389

Data are expressed as the median (25th to 75th percentile).

AIP-G indicates autoimmune pancreatitis-associated gastritis; AIP-G-HP(+), AIP-G without steroid therapy and with *Helicobacter pylori* infection; Eosino, eosinophil infiltration; IgG, immunoglobulin G; IgG4/IgG, IgG4-positive plasma cells/IgG-positive plasma cells ratio; IM, intestinal metaplasia; Lower, in the lower lamina propria; Mono, number of mononuclear cells; Neutro, neutrophil infiltration; Upper, in the upper lamina propria.

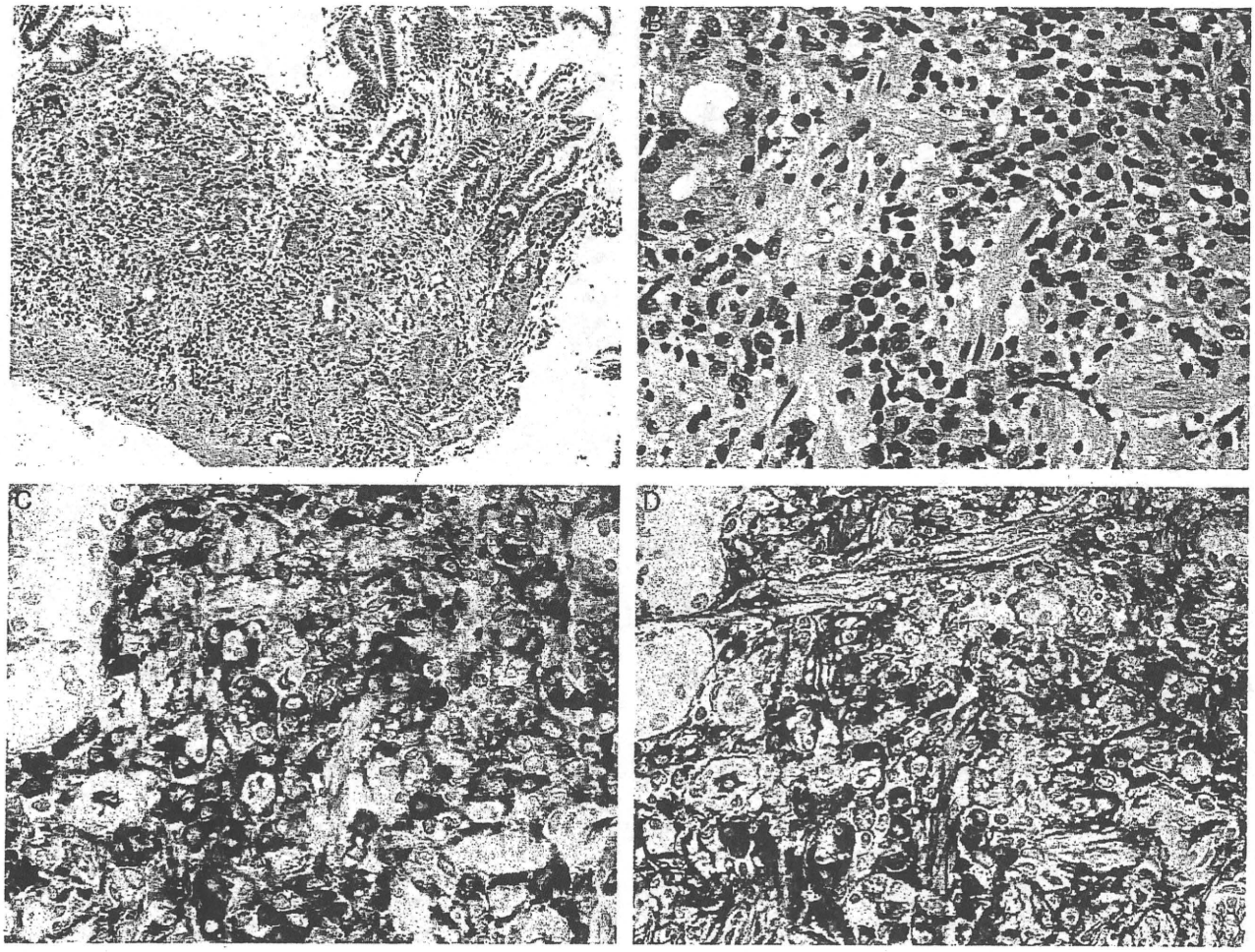

FIGURE 2. Stomach biopsy specimen of a patient with autoimmune pancreatitis-associated gastritis without steroid therapy and *Helicobacter pylori* infection. A, Inflammatory cell infiltration showing diffuse distribution in the fundic mucosa (HE staining, original magnification, 25 ×). B, Various degrees of lymphoplasmacytic and scattered eosinophil infiltration are found (HE staining, original magnification, 100 ×). Infiltration of (C) IgG-positive (immunostaining for IgG, original magnification, 100 ×) and (D) IgG4-positive plasma cells can be noted (immunostaining for IgG4, original magnification, 100 ×). HE indicates hematoxylin-eosin; IgG, immunoglobulin G.

infiltrates, intestinal metaplasia, and atrophy in the pyloric mucosa were mild and moderate, moderate, none and moderate, and mild and moderate, respectively. In the specimens obtained from 6 biopsy points of 1 patient of the AIP-G-ST(+) group, the distribution of inflammation was approximately uniform in the fundic and pyloric mucosa.

Immunohistochemical Findings

In the fundic mucosa of the AIP-G-HP(−) group, the IgG4/IgG ratio in the lower lamina propria was significantly higher than that in the upper lamina propria (Figs. 2C, D). In the fundic mucosa of the AIP-G-HP(+) group, the IgG4/IgG ratio in the lower lamina propria was higher than that in the upper lamina propria (Figs. 3C, D); however, the difference was not statistically significant. The IgG4/IgG ratios for the upper and lower lamina propria were not significantly different between the AIP-G-ST(−) groups. The IgG4/IgG ratios in the upper lamina propria in the AIP-G-ST(−) groups were significantly higher than those in the NSAID-G group. The IgG4/IgG ratios in the lower lamina propria in the AIP-G-ST(−) groups were significantly higher than those in the CAG and NSAID-G groups.

In the pyloric mucosa, in the AIP-G-ST(−) groups, the IgG4/IgG ratio in the lower lamina propria was significantly higher than that in the upper lamina propria. There was no significant difference in the IgG4/IgG ratios in the lower and upper lamina propria between the AIP-G-ST(−) groups. The IgG4/IgG ratios in the upper and lower lamina propria in the AIP-G-HP(−) groups were significantly higher than those in the NSAID-G group. The IgG4/IgG ratio in the upper lamina propria in the AIP-G-HP(+) group was significantly higher than that in the NSAID-G group. In the AIP-G-HP(+) group, the IgG4/IgG ratio in the lower lamina propria was higher than that in the NSAID-G group; however, the difference was not statistically significant. The IgG4/IgG ratios in

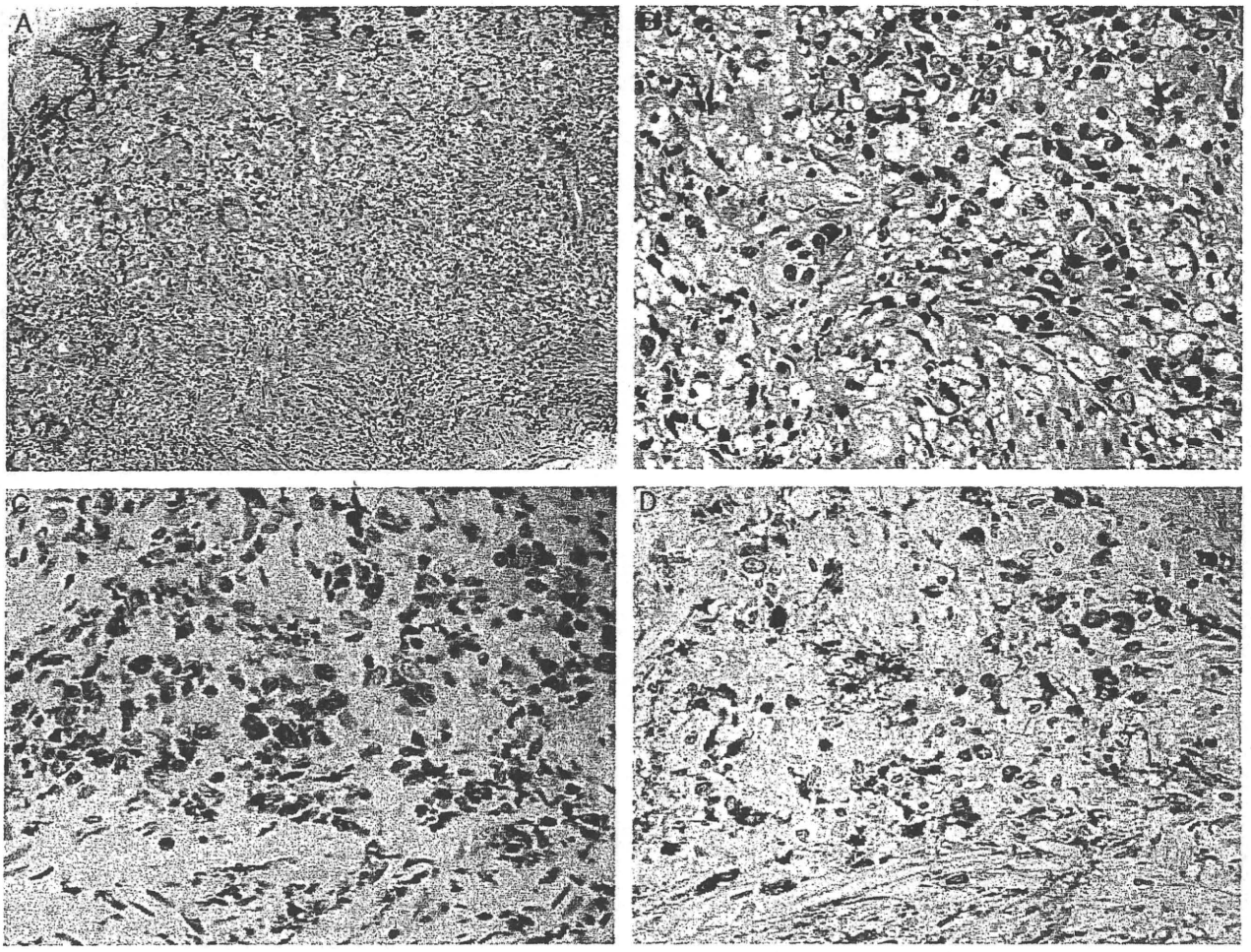

FIGURE 3. Stomach biopsy specimen of a patient with autoimmune pancreatitis-associated gastritis without steroid therapy and with *Helicobacter pylori* infection. A, Diffuse inflammatory cell infiltration is noted in the fundic mucosa (HE staining, original magnification, 25 ×). B, Various degrees of lymphoplasmacytic and scattered eosinophil infiltration are found. Fibrosis is also noted (HE staining, original magnification, 100 ×). Infiltration of (C) IgG-positive (immunostaining for IgG, original magnification, 100 ×) and (D) IgG4-positive plasma cells can be noted (immunostaining for IgG4, original magnification, 100 ×). HE indicates hematoxylin-eosin; IgG, immunoglobulin G.

the upper and lower lamina propria in the AIP-G-ST(−) groups were significantly higher than those in the CAG group.

In the AIP-G-ST(−) groups, the IgG4/IgG ratio in the upper and lower lamina propria were not significantly different between the fundic and the pyloric mucosa. In the specimens obtained from 6 biopsy points in the 3 patients of the AIP-G-ST(−) group, the distribution of the IgG4/IgG ratio in every case was approximately uniform in the fundic and the pyloric mucosa.

In the AIP-G-ST(+) group, the IgG4/IgG ratio in the fundic mucosa were 0.00 and 0.00 in the upper lamina propria and 0.21 and 0.00 in the lower lamina propria. In the AIP-G-ST(+) group, the IgG4/IgG ratio in the pyloric mucosa were 0.00 and 0.00 in the upper lamina propria and 0.00 and 0.00 in the lower lamina propria. In the fundic and the pyloric mucosa, the IgG4/IgG ratios in patients with AIP-G-ST(+) group were more discreet than those in the AIP-G-ST(−) group. In the specimens obtained from 6 biopsy points in 1 patient of the AIP-G-ST(+) group, the distribution of the IgG4/IgG ratio was approximately uniform in the fundic and the pyloric mucosa.

DISCUSSION

Characterization of variant forms of gastritis other than CAG, such as AIP-G, is important. This study revealed that AIP-G patients had lymphoplasmacytic and eosinophilic infiltration accompanied by the presence of many IgG4-positive plasma cells in the stroma and high serum IgG4 concentrations. The result of this study suggested that AIP-G had characteristics of IgG4-related disease and might be one of the IgG4-related sclerosing diseases.

In this study, although 1 patient with AIP-G-HP(−) had epigastralgia, he did not have HP infection. AIP-G-HP(−) patients did not have ulcers, but 2 of them

had erosion and 1 of them had redness. This finding contradicted the findings of Chang et al,[1] who reported that ulcer formation was a characteristic of AIP-G. This contradiction might be explained by the fact that most of the reported cases in that study had HP infection,[1,21] which may be associated with ulcer formation.

AIP-G has received worldwide recognition since it was first reported by Shinji et al[21] in 2004. Although many of their cases were accompanied with HP infection, they reported their pathologic findings as characteristic of AIP-G. They also reported that the inflammatory scores for AIP-G and CAG were not significantly different; however, in our study, eosinophil infiltration in the AIP-G patients was significantly higher than that in the CAG patients. Eosinophil infiltration is one of the most characteristic findings of IgG4-related sclerosing disease and is important in the diagnosis of AIP-G. No neutrophilic infiltration may also be a characteristic finding that distinguishes AIP-G as an IgG4-related sclerosing disease, provided HP infection is absent. Interestingly, the mononuclear cell density in the upper and lower lamina propria in the AIP-G-ST(−) groups was almost identical, but that in the upper lamina propria was higher than the corresponding value in the control groups. Diffuse mononuclear cell infiltration in the lamina propria might be another characteristic finding of AIP-G. The AIP-G-ST(−) groups had no difference in the degree of inflammation between the pyloric and the fundic mucosa, although inflammation is known to be significantly higher in the pyloric mucosa than in the fundic mucosa in CAG.[4]

Interestingly, much IgG4-positive plasma cells were observed a lot in the lower lamina propria than the upper propria in the AIP-G-ST(−) groups, irrespective of the HP status. In 1 patient with AIP-G-HP(+), diffuse fibrosis was observed in the lower lamina propria. These pathologic findings resembled those of IgG4-related sclerosing disease. The presence of gastric wall thickening and the accumulation of radioactive material on the stomach wall, which was revealed by Ga-67 citrate scintigraphy, indicated that there may be a marked inflammation in the deep gastric wall. This might explain the absence of significant changes on the gastric surface mucosa during the endoscopic examinations of AIP-G patients. Further studies must be conducted to elucidate the clinicopathologic characteristics of AIP-G.

Many studies suggest that not only the number of IgG4-positive plasma cells but also the IgG4/IgG ratio is important for the diagnosis of extrapancreatic IgG4-related sclerosing disease.[30,31] An IgG4/IgG ratio of greater than 40% to 50% usually seems to be highly suggestive of IgG4-related disease. In this study, the IgG4/IgG ratio in the lower lamina propria of fundic mucosa was more than 50%. Sepehr et al[20] reported that the cut-off value for the IgG4/IgG ratio in the Vater papilla of an AIP patient was 0.1. Although the IgG4/IgG ratio in almost all the AIP-G-HP(+) patients was more than 0.1, we could not distinguish whether this inflammation was caused by HP infection or AIP-G. However, the IgG4/IgG ratio in the AIP-G-HP(−) patients suggests that AIP-G could have caused the stomach inflammation, even in the absence of HP infection. It is also important to note that patients without HP infection may have gastritis resembling pancreatic inflammation observed in AIP.

Steroid therapy is effective against IgG4-related sclerosing disease,[28] as the IgG4/IgG ratios in the AIP-G-ST(+) group were predominantly lower than those in the AIP-G-ST(−) groups. AIP-G may also be effectively treated using steroid therapy. But the symptoms in the AIP-G-ST(+) group did not alleviate after steroid therapy; this could be because some clinical findings associated with HP infection persisted.

In summary, AIP-G is also one of the IgG4-related sclerosing diseases, and the IgG4/IgG ratio is a useful marker for further research on IgG4-related sclerosing diseases.

ACKNOWLEDGMENTS

The authors thank Dr Yoh Zen (Department of Human Pathology, Kanazawa University Graduate School of Medicine and Division of Pathology, Kanazawa University Hospital) for his advice and encouragement. They are also grateful to Masanobu Momose, Yasuyo Shimojo, Mieko Horikawa, Yayoi Uehara, Megumu Kubota, and Masaomi Takahashi (Shinshu University Hospital) for their excellent technical assistance.

REFERENCES

1. Chang MC, Chang YT, Wei SC, et al. Autoimmune pancreatitis associated with high prevalence of gastric ulcer independent of *Helicobacter pylori* infection status. *Pancreas*. 2009;38:442–446.
2. Deshpande V, Mino-Kenudson M, Brugge W, et al. Autoimmune pancreatitis: more than just a pancreatic disease? A contemporary review of its pathology. *Arch Pathol Lab Med*. 2005;129:1148–1154.
3. Dixon MF, Genta RM, Yardley JH, et al. Classification and grading of gastritis. The updated Sydney System. International Workshop on the Histopathology of Gastritis, Houston 1994. *Am J Surg Pathol*. 1996;20:1161–1181.
4. Goldstone AR, Quirke P, Dixon MF. *Helicobacter pylori* infection and gastric cancer. *J Pathol*. 1996;179:129–137.
5. Group TES. Epidemiology of, and risk factors for, *Helicobacter pylori* infection among 3194 asymptomatic subjects in 17 populations. The EUROGAST Study Group. *Gut*. 1993;34:1672–1676.
6. Hamano H, Kawa S, Horiuchi A, et al. High serum IgG4 concentrations in patients with sclerosing pancreatitis. *N Engl J Med*. 2001;344:732–738.
7. Hamano H, Kawa S, Ochi Y, et al. Hydronephrosis associated with retroperitoneal fibrosis and sclerosing pancreatitis. *Lancet*. 2002; 359:1403–1404.
8. Hirano K, Kawabe T, Komatsu Y, et al. High-rate pulmonary involvement in autoimmune pancreatitis. *Intern Med J*. 2006;36:58–61.
9. Ito T, Nakano I, Koyanagi S, et al. Autoimmune pancreatitis as a new clinical entity. Three cases of autoimmune pancreatitis with effective steroid therapy. *Dig Dis Sci*. 1997;42:1458–1468.
10. Kamisawa T, Funata N, Hayashi Y, et al. A new clinicopathological entity of IgG4-related autoimmune disease. *J Gastroenterol*. 2003;38:982–984.
11. Kamisawa T, Funata N, Hayashi Y, et al. Close relationship between autoimmune pancreatitis and multifocal fibrosclerosis. *Gut*. 2003;52:683–687.
12. Kanno A, Satoh K, Kimura K, et al. Autoimmune pancreatitis with hepatic inflammatory pseudotumor. *Pancreas*. 2005;31:420–423.